

# Long duration of benthic ecological recovery from the early Toarcian (Early Jurassic) mass extinction in the Cleveland Basin, UK



Jed W. Atkinson, Crispin T. S. Little\* and Alexander M. Dunhill

School of Earth and Environment, University of Leeds, Leeds LS2 9JT, UK

JWA, 0000-0003-4042-2489; CTSL, 0000-0002-1917-4460; AMD, 0000-0002-8680-9163

\* Correspondence: [earctsl@leeds.ac.uk](mailto:earctsl@leeds.ac.uk)

**Abstract:** The Cleveland Basin of Yorkshire, UK hosts one of the most iconic Lower Jurassic rock successions for studying the Toarcian oceanic anoxic event and the associated mass extinction, yet our understanding of the subsequent ecological recovery is limited. This study documents for the first time the full extent and nature of benthic macrofaunal recovery from the early Toarcian mass extinction event within the Cleveland Basin. Benthic oxygen levels remained low following the extinction event, allowing specialist communities that were tolerant to low oxygen levels to dominate. Recovery began properly once the seafloor ventilation had begun to improve and was first expressed by an expanded ecological tiering structure. Recovery progressed slowly thereafter with the possible return to oxygen-restricted environments. As sea-levels fell and sand-dominated deposition again occurred within the basin, the recovery accelerated, with ecological and species richness being reattained and even exceeding pre-extinction levels. Full recovery occurred, at the latest, *c.* 7 myr after the extinction event; this duration is on par with estimates of recovery rates from the largest mass extinction event of the Phanerozoic (the end-Permian mass extinction event). Recovery within the Cleveland Basin was likely to have been strongly influenced by local sea-levels and the continuation of challenging environmental conditions after the extinction event.

**Supplementary material:** Benthic fossil occurrence data are available at <https://doi.org/10.6084/m9.figshare.c.6332986>

**Received** 20 August 2022; **revised** 23 November 2022; **accepted** 29 November 2022

Recovery intervals are crucial periods of biotic change that allow new groups to radiate into the emptied ecospace after extinction events (Erwin *et al.* 1987; Kauffman and Erwin 1995; Harries *et al.* 1996; Kauffman and Harries 1996; Solé *et al.* 2002; Twitchett 2006). However, the definition of this post-extinction period is highly dependent on the scale and groups of organisms studied (Danise *et al.* 2015; Dai *et al.* 2018; Song *et al.* 2018; Atkinson and Wignall 2019). Different groups display different post-extinction diversity dynamics due to their intrinsic evolutionary rates, which means that recovery of the whole ecosystem will take longer than the recovery of one clade alone (Stanley 2009; Guex *et al.* 2012; Song *et al.* 2016; Dai *et al.* 2018). The complexity of ecosystems is also important because local environments may be more susceptible to environmental change and may perpetuate adverse conditions (Sheehan 1985; Stanley 1988; Atkinson and Wignall 2019; Müller *et al.* 2020).

It is important to define what is meant by ecological recovery and several models have been developed to do so. Such models use a variety of metrics to document the overall ‘healthiness’ of a community, typically including a measure of the number of species present in different intervals. This can be measured through horizon-level or time-binned species counts (e.g. Hallam 1987; Mander *et al.* 2008; Pugh *et al.* 2014). This is a distinctly different measure of diversity from another commonly used metric – evenness, or conversely, dominance – which measures the ratio between each species to determine whether an assemblage is numerically dominated by a small number of species (Schubert and Bottjer 1995; Twitchett 2006; Danise *et al.* 2013). A third common component of recovery models is to include a measure of ecological diversity. This may be the number of different life modes present and the number of species or specimens that occupy it.

Twitchett (2006) found that the levels inhabited by organisms relative to the seafloor (ecological tiering) was a good indicator for recovery (Fig. 1). This includes burrowers at different depths (deep or shallow infaunal), organisms that sit low on the surface of the sediment (low-level epifaunal) and organisms that reach up into the water column from the seafloor, such as corals or crinoids (erect epifaunal). Following a mass extinction event, ecological tiering collapses, leaving communities dominated by low-level epifaunal organisms (Twitchett 1999). Another method often used in recovery studies is a measure of body size (Urbanek 1993; Payne 2005; Atkinson and Wignall 2020). In the aftermath of mass extinctions, organisms tend to be of diminutive stature due to either high rates of juvenile mortality or small adult body sizes; the return to large body sizes can be seen as a sign that the ecosystem has recovered (e.g. Atkinson and Wignall 2020).

Kauffman and Erwin (1995) divided the post-extinction interval into two distinct phases: the survival interval and the recovery interval (Fig. 1). The former is characterized by low taxonomic richness with fossil communities dominated, in terms of specimens, by a handful of small-sized species that occupy low levels of ecological tiering (e.g. low-level epifaunal). Such species are usually inferred to have been disaster taxa and opportunists that were likely R strategists – attaining sexual maturity rapidly and giving rise to large numbers of offspring (Guex 1992; Harries *et al.* 1996). The succeeding recovery interval of Kauffman and Erwin (1995) is characterized by a period of increasing taxonomic richness, with new species arising from surviving lineages and species migrating into the area from theorized refugia.

The model for post-extinction recovery of Twitchett (2006), which is based on the end-Permian mass extinction event, incorporates key ichnotaxa and has additional ecological parameters

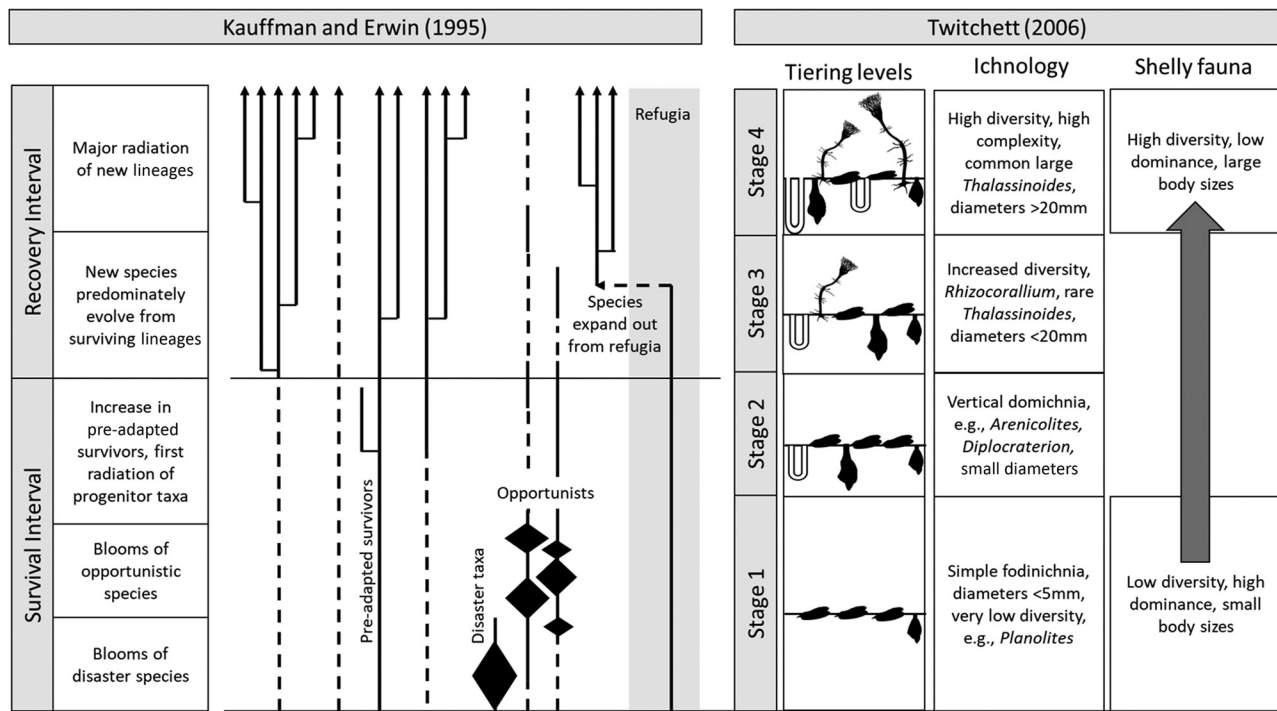


Fig. 1. Comparative summaries for the Kauffman and Erwin (1995) and Twitchett (2006) recovery models.

in four post-extinction phases (Fig. 1). The first equates to the survival interval of Kauffman and Erwin (1995), but includes a depauperate trace fossil assemblage. It is less clear how the second stage of recovery in the Twitchett (2006) model may relate to the Kauffman and Erwin (1995) model; it may be equivalent to the latest survival interval or the earliest recovery interval (Fig. 1). Subsequent phases are equivalent to the recovery interval of Kauffman and Erwin (1995), but Twitchett (2006) dilutes the importance of species richness alone by including the community structure, body size and morphological complexity (Fig. 1). This later model includes the expansion of seafloor tiering and the repopulation of ecological niches. Ecosystems in the aftermath of a mass extinction event have been likened to a ship sailed by a skeleton crew (Foster and Twitchett 2014), in that all ecological roles are present, but with each life mode represented by only one or two species. Consequently, species diversity remains low, while ecological diversity appears to be unaffected.

Post-extinction recovery has been best studied for the Permian–Triassic, end-Triassic and Cretaceous–Paleogene extinction events (Hallam 1987; Hansen 1988; Nützel 2005; Barras and Twitchett 2007; Hautmann *et al.* 2008; Sessa *et al.* 2009; Hu *et al.* 2011; Ros *et al.* 2011; Chen and Benton 2012; Aberhan and Kiessling 2014; Pugh *et al.* 2014; Damborenea *et al.* 2017; Foster and Sebe 2017; Dunhill *et al.* 2018; Song *et al.* 2018; Alvarez *et al.* 2019; Atkinson and Wignall 2019, 2020; Whittle *et al.* 2019). By comparison, recovery following second-order mass extinction events, such as that of the early Toarcian (Early Jurassic), is less well understood. The early Toarcian event was associated with the onset of a globally occurring negative carbon isotope excursion, produced by the release of isotopically light CO<sub>2</sub> by the Karoo–Ferrar large igneous province (Palfy and Smith, 2000) and/or methane hydrates (Hesselbo *et al.* 2000; Kemp *et al.* 2005), warming of 5–10°C (Bailey *et al.* 2003; Ruebsam *et al.* 2019), an enhanced hydrological cycle (Bailey *et al.* 2003), marine transgression (Hallam and Wignall 1999) and the Toarcian oceanic anoxic event (TOAE; Jenkyns 1988), which was largely a regional phenomenon.

The TOAE was particularly well developed in the epicontinental basins of NW Europe, with the deposition in the Serpentinum Zone

of finely laminated, organic-rich (black) shales, such as the Schistes Carton of France, the Posidonia Shale of Germany and the Mulgrave Shale (formerly the Jet Rock) of northern England (Jenkyns 1988). Within these restricted basins of NW Europe, the TOAE is thought to have been the main cause of the early Toarcian mass extinction event, especially for benthic faunas, because the extinction level is coincident with the beginning of black shale deposition at the end of the Tenuicostatum Zone (Little 1995; Little and Benton 1995; Schmid-Röhl *et al.* 2002; Wignall *et al.* 2005; Caswell *et al.* 2009; Danise *et al.* 2013, 2015; Caswell and Frid 2017). In other regions, such as the Sub-Boreal and Tethyan realms, these oxygen-restricted facies were weakly or not at all developed during the Toarcian and, instead, a rapid increase in temperature may have been the main driver of extinction (e.g. McArthur *et al.* 2008; Gómez and Goy 2011; Baeza-Carratalá *et al.* 2015; Miguez-Salas *et al.* 2017; Danise *et al.* 2019). Earlier extinctions occurred at the Pliensbachian–Toarcian boundary in ammonites (Dera *et al.* 2010; Caruthers *et al.* 2013) and in Tethyan coral faunas (Vasseur *et al.* 2021), the cause(s) of which may have been warming from the first major eruptive phase of the Karoo–Ferrar large igneous province (Caruthers *et al.* 2013; Percival *et al.* 2015).

Early studies on extinction and recovery spanning the Pliensbachian and Toarcian stages were conducted at low resolution, with the species counts compiled by ammonite zone across much of Europe (Hallam 1976, 1986, 1987, 1996). These studies showed a delayed recovery among the bivalves (with species richness beginning to approach pre-extinction values by the latest Toarcian), whereas the brachiopods displayed little to no recovery within the studied time interval. Similar recovery patterns were found in more recent regional studies from the NW Caucasus (Ruban 2004), the Boreal–Arctic region (Zakharov *et al.* 2006) and in the Andean Basin of Chile (Aberhan and Fürsich 2000), with the latest Toarcian diversity not regaining its pre-extinction richness. However, the ecological structure of mid Toarcian bivalve assemblages within the Andean Basin attained a level of ecological complexity similar to that of the late Pliensbachian, despite a lower species richness (Aberhan and Fürsich 2000). Recovery occurred at a greater rate within the shallow water succession of northern and

central Spain, where brachiopods recovered their diversity and body size by the Variabilis Zone (García Joral and Goy 2009; García Joral *et al.* 2011, 2018) or, locally, earlier still during the Serpentinum Zone (Danise *et al.* 2019). This ‘enhanced’ recovery was likely linked to the absence of marine oxygen depletion (García Joral and Goy 2009; García Joral *et al.* 2011; Danise *et al.* 2019).

The Cleveland Basin (northern UK) was home to high-diversity benthic fossil assemblages in the late Pliensbachian, with most species being evenly represented (no one species dominated) and featuring a wide range of ecological groups occupying all levels of benthic tiering (Little 1995; Caswell *et al.* 2009; Danise *et al.* 2013; Caswell and Frid 2017). Although there was an extinction event in ammonites at the Pliensbachian–Toarcian boundary (the loss of the family Amaltheidae, which defines the end of the Pliensbachian; Howarth 1955), most of the benthic taxa passed through into the early Toarcian unaffected.

The benthic extinction horizon occurred within a few metres of the sedimentary section in the Semicelatum Subzone of the Tenuicostatum Zone at *c.* 183 Ma (Fig. 2), leading up to the first appearance of thick laminated black shales (Little and Benton 1995; Caswell *et al.* 2009; Danise *et al.* 2013; Caswell and Frid 2017). With the black shales of the succeeding Serpentinum Zone, there was a marked shift in the structure of the benthic assemblages, with a collapse of the benthic tiering structure (only low-level epifauna remained) and assemblages dominated by large numbers of the opportunistic, and probable low-oxygen specialist, bivalves *Pseudomytiloides* and *Bositra* (Little 1995; Danise *et al.* 2013; Caswell and Dawn 2019). At the same time, sphaeromorph- and *Tasmanites*-dominated plankton communities replaced earlier dinoflagellate communities (Slater *et al.* 2019; Danise *et al.* 2022).

The benthic faunal diversity remained low well into the Commune Subzone of the Bifrons Zone, *c.* >2 myr after the extinction horizon (Fig. 2), despite the negative carbon isotope excursion lasting only *c.* 0.9 myr (Suan *et al.* 2008). The Commune Subzone records the onset of the recovery, as documented by the first appearance of shallow and deep infaunal tiering. The return of infaunal species marked the loss of well-laminated mudstone and is represented by a bloom of the deposit-feeding bivalve *Dacryomya ovum* (Little 1995; Caswell *et al.* 2009; Danise *et al.* 2013; Caswell and Dawn 2019). Other new species arose from surviving lineages, such as the deep infaunal suspension-feeding bivalve *Gresslya donaciformis* (Little 1995; Caswell *et al.* 2009; Danise *et al.* 2013).

Epifaunal tiering increased shortly afterwards, with the first post-extinction occurrence of crinoids (Little 1995). Although plankton communities returned to dinoflagellate-dominated assemblages within the Bifrons Zone (Slater *et al.* 2019; Danise *et al.* 2022), neither trace nor body fossil diversity (both taxonomic and functional) had returned to pre-extinction levels at that time (Little 1995; Little and Benton 1995; Martin 2001, 2004; Danise *et al.* 2013, 2022; Caswell and Frid 2017).

All previous studies of extinction and recovery during the Toarcian in the Cleveland Basin have their upper limits near the top of the Bifrons Zone because the succeeding ammonite zones of the Middle and Upper Toarcian were removed by later Mid-Jurassic erosion at most of the Yorkshire sections (Knox 1984; Milsom and Rawson 1989; Little 1995; Caswell *et al.* 2009; Powell 2010; Danise *et al.* 2013), meaning that our knowledge of the recovery pattern from the early Toarcian extinction event is incomplete. However, there is one section on the North Yorkshire coast, at Ravenscar, where a near-complete middle and upper Toarcian section crops out in the cliffs and foreshore (Dean 1954; Knox 1984; Powell 1984). A few studies have sampled this section for palynology (Riding 1984), trace fossil assemblages (Martin 2001, 2004) and geochemical data (Newton *et al.* 2011), but all at relatively low resolution. Here, we report a high-resolution sampling study of benthic macrofossils through the middle and upper Toarcian from the Ravenscar section using similar methodologies to the previous studies of Little (1995) and Danise *et al.* (2013). We incorporate new and existing data to produce new species ranges and palaeoecological data for the entire late Pliensbachian to Toarcian time interval in the Cleveland Basin.

## Geological setting

During the Jurassic, the Cleveland Basin consisted of a series of small extensional basins within a shallow epicontinental seaway (Powell 2010). The oldest unit within this study area is the Staithes Sandstone Formation of the Pliensbachian Stage (Powell 1984). This fine- to medium-grained sandstone is interpreted as storm wave-influenced, sublittoral and shoreface sands (Howard 1984; Powell 2010). This is followed by the Cleveland Ironstone Formation, which is divided into the Penny Nab and Kettleless members (Powell 1984; Howard 1985). This formation consists of cyclical rhythms of chamosite-oidal ironstone seams, mudstones and sandstones,

Epoch	Stage	Formation/Member		Zone/Subzone		Age (Ma)	
Mid. Jur.	Aalenian	Dogger		?Opalinum		174.8	
Lower Jurassic	Toarcian	Blea Wyke Sandstone	Yellow Sandstone	Aalensis	?Fluitans	176.0	
				Pseudoradiosa	?Pseudoradiosa		
			Grey Sst.	Dispansum	?Gruneri	177.2	
			Fox Cliff Silt.	Thouarsense	?Insigne	177.6	
		Whitby Mudstone	Peak Mudstone	Variabilis	Fallaciosum	Striatulum	178.3
					?Vitiosa	Illustris	
			Alum Shale	Bifrons	Variabilis	Variabilis	179.8
					Crassum	Fibulatum	
					Commune	Falciferum	
					Exaratum	Semicelatum	
		Mulgrave Sh.	Serpentinum	Tenuicostatum	Tenuicostatum	Clevelandicum	181.2
					Paltum	Paltum	
					Hawskerense	Apyrenum	
					Gibbosus	Subnodosus	
Pliensbachian	Cleveland Ironstone	Kettleless	Spinatum	Stokesi	183.2		
				Penny Nab		Margaritatus	
		Penny Nab	Margaritatus	Margaritatus		Stokesi	184.2
						Stokesi	

Fig. 2. Outline of the lithostratigraphy and biostratigraphy of the Cleveland Basin. Age model from Gradstein *et al.* (2020). Sh, Shale; Silt, Siltstone; SSt, Sandstone.

which may have been influenced by glacio-eustasy (Howarth 1955; Howard 1985; Korte and Hesselbo 2011). These sediments are thought to have been deposited within a sediment-starved, laterally extensive shallow lagoon or littoral sea (Powell 2010).

Following the Cleveland Ironstone, a marine transgression resulted in the deposition of the Whitby Mudstone Formation, around the Pliensbachian–Toarcian boundary (Powell 1984). This argillaceous unit is represented in most coastal sections by three members: the Grey Shale; the Mulgrave Shale (formerly the Jet Rock Member of Powell 1984); and the Alum Shale (Fig. 2). The Mulgrave Shale Member has the greatest total organic carbon content of the sequence and represents the peak transgression (Hallam 1997; McArthur *et al.* 2008; Pearce *et al.* 2008). The water depth has been estimated at 50–100 m, although this was likely to have been towards the shallower estimate (Hallam 1997; Wignall *et al.* 2005; Powell 2010).

Marine regression began during deposition of the Alum Shale Member (Powell 2010). Across much of the Cleveland Basin, the Alum Shale Member is truncated in the Crassum Subzone of the Bifrons Zone by a period of Mid-Jurassic erosion. However, a more complete section is preserved within the Peak Trough Member (Fig. 3), which was actively subsiding during the Jurassic (Milsom and Rawson 1989), and this upper Toarcian section is exposed in the cliffs and wave-cut platforms near Ravenscar, 6 km south of Robin Hood's Bay (Fig. 3). This succession includes the uppermost members of the Whitby Mudstone Formation: the topmost Alum Shale, the Peak Mudstone and the Fox Cliff Siltstone members (Fig. 2). As the names of these members indicate, they exhibit an increasing grain size and are a continuation of a regressive sequence (Knox 1984).

In the Ravenscar section, the Whitby Mudstone Formation grades upwards into the Blea Wyke Sandstone Formation (Knox 1984). This formation is separated into the Grey and the Yellow Sandstone members (Knox 1984), the contact between the two forming a sharp colour change in the cliff running from Ravenscar to Blea Wyke. The Grey Sandstone Member has a higher mud content and features hard siderite-rich horizons, whereas the Yellow Sandstone Member is a cleaner sandstone. Both members are intensely bioturbated and their deposition occurred within the sublittoral zone, above the wave base (Knox 1984).

## Materials and methods

During the summers of 2013 and 2017, we collected from 37 sample horizons, spaced mostly at 1 m intervals (range 0.5–4 m due to differences in rock availability), from 45 m of the middle and upper Toarcian stratigraphy, from the topmost Alum Shale Member (Bifrons Zone) to the top of the Yellow Sandstone Member (Aalensis Zone) in the cliff and foreshore exposures between Ravenscar and Blea Wyke Point, North Yorkshire (54° 23' 58" N,

00° 28' 33" W) (Fig. 3). The sedimentary logs of Howarth (1962), Knox (1984) and Dean (1954) were used to locate the sample points in the stratigraphic section. At each sample horizon, *c.* 1 kg of bulk rock was collected and the benthic species richness and abundances were counted from wave-cut platforms (where available) or cliff exposure, for up to 2 h per horizon.

The bulk samples were taken back to the University of Leeds and broken using a hammer and chisel to expose their benthic fossil content. The bulk samples gave species diversity and abundance data from equal rock volumes. Counts were made in the field from wave-cut platforms and cliff sections to increase the size of the available dataset for a total evidence approach. These datasets were plotted separately as a test of sampling bias due to differences in exposure quality, but were combined for the range chart and palaeoecological analysis.

For brachiopods and bivalves, the number of individuals was determined by counting the sum of articulated and disarticulated valves. For gastropods and scaphopods, single shells were counted as one individual. For crustaceans, cephalothorax specimens were counted as one individual and, for crinoids, discrete clusters of ossicles were considered as one individual. Fossils in the Yellow Sandstone Member are largely preserved as moulds, so the surfaces of the bulk-rock samples from this unit were cast using silicone rubber and these casts were used to identify the fossils. Benthic tiering and feeding strategies were assigned using the scheme from Bambach *et al.* (2007; see Supplementary Material). Trace fossil occurrences for the Ravenscar section were taken from Martin (2001).

Benthic species richness and abundance counts from the Ravenscar section were combined with those of Danise *et al.* (2013) to form a dataset spanning the late Pliensbachian Staithes Sandstone Formation to the Blea Wyke Sandstone at the top of the Toarcian. It is important to note that Danise *et al.* (2013) used a larger rock volume (3 kg) for their bulk samples. This combined dataset was used to construct species range charts for that time interval, with range extensions from younger and older units in the basin taken from previously published work (Sowerby 1821; Morris and Lycett 1854; Tate and Blake 1876; Dean 1954; Howarth 1962, 1992; Hallam 1967; Howard 1984, 1985; Johnson 1984; Simms 1989; Ager 1990; Doyle 1990; Caswell *et al.* 2009; Atkinson and Wignall 2020). Combined species richness data (bulk + foreshore) were subsampled to standardize species richness on the basis of the number of fossil occurrences (Dunhill *et al.* 2018). Subsampling quotas were set at 50 occurrences per sampled horizon and any of these that did not meet this quota was omitted. In each case, subsampling was carried out across 1000 iterations. Simpson's index of diversity 1-D (SID) was used to assess the evenness of benthic assemblages per sample horizon for the full dataset, following the methods used in Danise *et al.* (2013). This returns a result between 0 and 1, where 0 is an assemblage

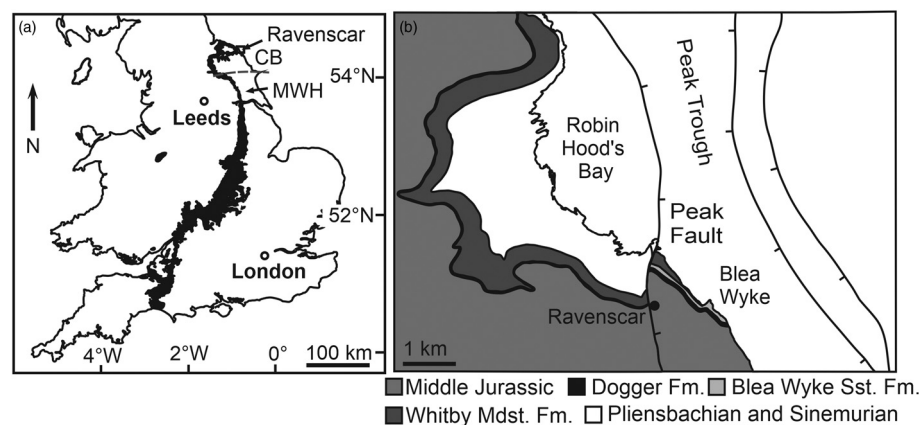


**Fig. 3.** (a) Map showing location of Lower Jurassic outcrops in England and Wales (after Gründel *et al.* 2011). (b) Detailed location map showing key lithological units and structures in the study area. CB, Cleveland Basin; Fm., Formation; Mdst., Mudstone; MWH, Market Weighton High; SSt., Sandstone.

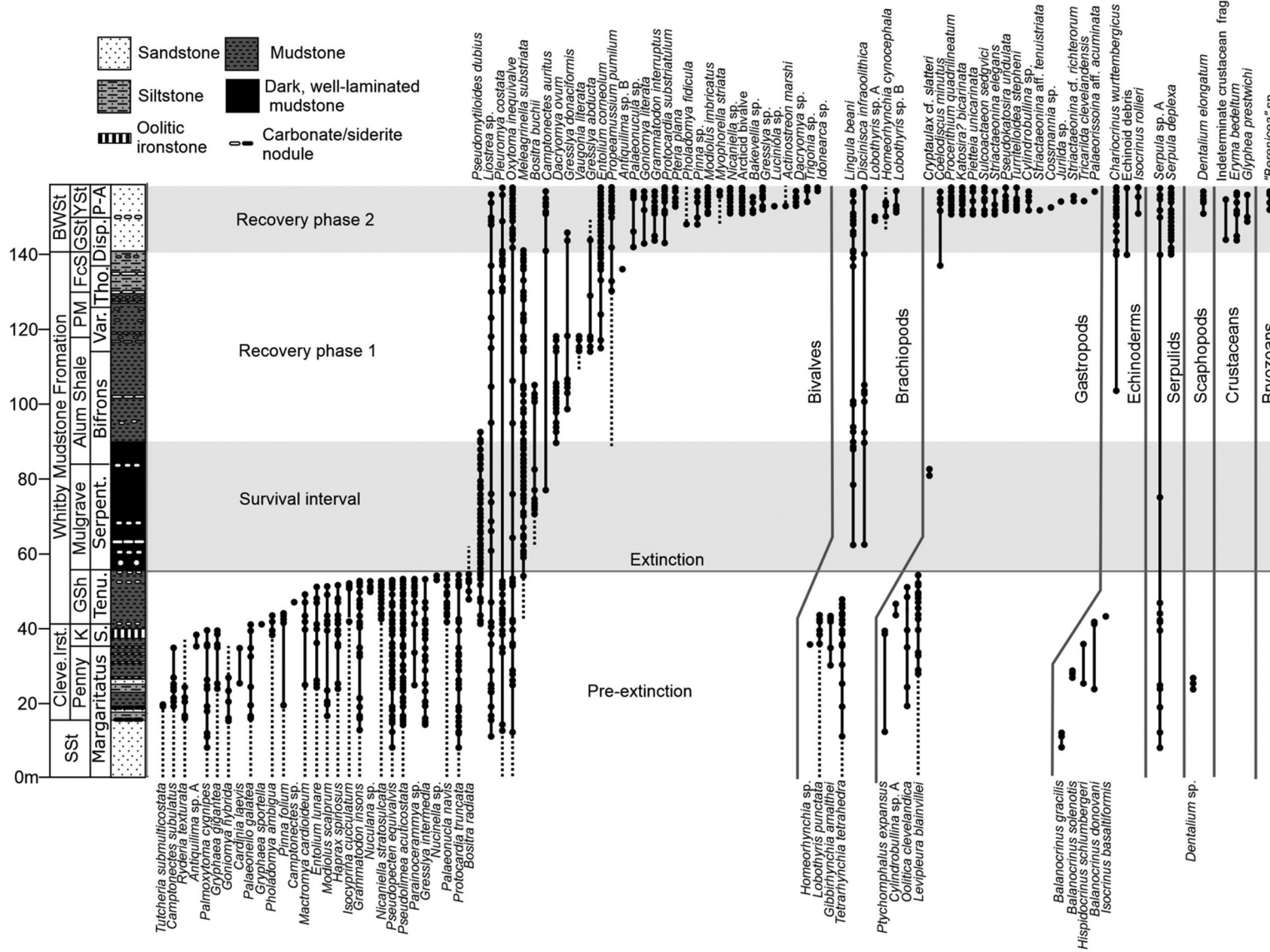


**Fig. 4.** Species occurrence range chart for bivalves, brachiopods, gastropods, echinoderms, serpulids, scaphopods, crustaceans and bryozoans. The closed circles indicate horizons where species were found, the solid lines connect occurrences and the dashed lines depict species ranges from previously published work (see methods section for details). SSt, Staithees Sandstone Formation; Cleve. Irst., Cleveland Ironstone Formation; BWSt, Blea Wyke Sandstone Formation; Penny, Penny Nab Member; K, Kettleless Member; GSh, Grey Shale Member; Mulgrave, Mulgrave Shale Member; PM, Peak Mudstone Member; FcS, Fox Cliff Siltstone Member; GST, Grey Sandstone Member; YSt, Yellow Sandstone Member; S., Spinatum Zone; Tenu., Tenuicostatum Zone; Var., Variabilis Zone; Tho., Thoarsense Zone; Disp., Dispansum Zone; P-A, Pseudoradiosa Zone to Aalensis Zone.

dominated by a single species and 1 means all species are equally represented.

To study the ecological composition from sample horizons, we constructed percentage area plots for the 11 identified benthic palaeoecologies (erect epifaunal suspension feeders, low-level epifaunal suspension feeders, epifaunal grazers, epifaunal predators, semi-infaunal suspension feeders, semi-infaunal predators, shallow infaunal suspension feeders, shallow infaunal deposit feeders, shallow infaunal/epifaunal microcarnivores, shallow infaunal species with chemosymbionts and deep infaunal suspension feeders). Proportional diversity was assessed within the orders of bivalves, using raw species counts with taxonomic information from Cox *et al.* (1969).

An absolute timescale is provided from Gradstein *et al.* (2020) using dated ammonite zone boundaries (Fig. 2). For the upper Toarcian, the ammonite zone schemes of Knox (1984) and Dean (1954) have been correlated to the current scheme presented in Page (2003), which was used by Gradstein *et al.* (2020). As many old subzones have since been elevated to zones, there is a good correspondence for most of the zonal biostratigraphy of the Ravenscar succession. However, determining the position of some subzones is more problematic and it is necessary to detail a few points where the correlation between the schemes was not straightforward.

There is no evidence for the Fluitans Subzone on the Yorkshire Coast, so it seems likely that this was removed by Mid-Jurassic erosion below the 'Terebratula beds' that mark the base of the Dogger Formation (Dean 1954). The Mactra Subzone is indicated by the presence of a single *Dumortiera moorei* specimen found by Dean (1954) in the upper half of the Yellow Sandstone Member. The Pseudoradiosa Subzone is unconfirmed, but there is no sedimentary evidence for a break in deposition to suggest that it is not present. It is likely, instead, that the poor state of preservation of ammonites from this part of the section is the reason for this subzone not being recorded. Indeed, we collected several ammonites belonging to the genus *Hudlestonia* from the upper half of the Yellow Sandstone Member, but none that could be identified to species level and therefore used for biostratigraphy. The Dispansum Subzone of Knox (1984) and Dean (1954) corresponds well with the Dispansum Zone of Page (2003) and is confirmed by the presence of *Phlyseogrammoceras dispansum*, the index taxa for the Dispansum Zone, from much of the Grey Sandstone Member (Dean 1954). Despite this, the Gruner and Insigne subzones of the Dispansum Zone were not confirmed. There is no record of the index ammonites from the Vitiosa Subzone, although this may be due to poor accessibility towards the top of the Peak Mudstone Member. The index ammonites for the Illustris Subzone were recorded in the Peak Mudstone by Dean (1954).

## Results

In total, 23 345 benthic macrofossil specimens were counted from 37 sample horizons in the Ravenscar section. When combined with data from Danise *et al.* (2013), this gave a total of 35 615 benthic fossils from 219 sample horizons (Figs 4–6). On the basis of the range charts and palaeoecological analysis, we distinguish four phases related to benthic extinction and recovery in the Cleveland Basin: (1) the pre-extinction interval (Margaritatus Zone to *Tenuicostatum* Zone); (2) the immediate post-extinction interval (*Tenuicostatum* Zone, *Semicelatum* Subzone to *Bifrons* Zone, *Commune* Subzone) represented by the communities tolerant to low oxygen levels; (3) the early phase recovery interval (*Bifrons* Zone, *Commune* Subzone to *Dispansum* Zone) defined by the reappearance of ecologies that were exclusively lost from the basin at the extinction horizon; and (4) the late phase recovery interval (*Dispansum* Zone to *Aalensis* Zone), when the

species richness increased markedly and populated ecological niches.

### **Pre-extinction interval: *Margaritatus* Zone to *Tenuicostatum* Zone**

Prior to the extinction event, the species richness was highly variable, reaching highs of 20 species per sample horizon (Fig. 5a). On average, these sample horizons record six benthic ecological life modes, with low-level epifaunal suspension feeders being the most diverse (up to ten species from one sample point), but also a rich infaunal diversity with up to three deep infaunal species and four shallow infaunal species from a single sample horizon (Fig. 7). Towards the extinction event, there was a gradual decrease in the abundance of deep infaunal suspension feeders (Danise *et al.* 2013). Immediately prior to the extinction event, shallow infaunal deposit-feeding bivalves, such as *Palaeonucula navis*, form a significant proportion of these assemblages and, for a short interval straddling the extinction event, the bivalve *Nucinella* sp. is briefly abundant, forming up to 79% of the benthos in specific horizons (Danise *et al.* 2013; Caswell and Frid 2017).

### **Immediate post-extinction interval: *Tenuicostatum* Zone, *Semicelatum* Subzone to *Bifrons* Zone, *Commune* Subzone**

Following the extinction event, species richness sharply decreased to typically two species and remained low throughout much of this time. During the deposition of laminated black shales, a distinctive series of fossil assemblages were present, formed of low-level epifaunal suspension feeders with an abundance of individuals. Monospecific shell pavements of the 'paper pecten' *Bositra radiata* occur near the top of the Grey Shale Member in the *Semicelatum* Subzone (Little 1995; Caswell and Coe 2013; Danise *et al.* 2015). These bivalves have valves up to 50 mm in height (Little 1995). *B. radiata* was found in only a narrow stratigraphic interval in the Grey Shale Member, although Caswell *et al.* (2009) report a transient reoccurrence of the species higher in the Mulgrave Shale, from the upper *Exaratum* Subzone, *Serpentinum* Zone.

Above this level, in the *Falciferum* Subzone (*Serpentinum* Zone), *Bositra buchii* occurs in thin, monospecific shell beds. This species is smaller than *B. radiata*, with a maximum shell height of c. 10 mm. *Pseudomytiloides dubius* occurs sporadically in low numbers throughout the Grey Shale Member, but dominates the benthic fauna in the organic-rich facies of the Mulgrave Shale, forming thin shell beds restricted to discrete horizons. These shell beds occasionally also contain a few individuals of *Meleagrinnella substriata* and *B. buchii* (Caswell and Coe 2013; Danise *et al.* 2015). These assemblages gradually disappear in the lower Alum Shale Formation, with *P. dubius* last recorded from the *Commune* Subzone (*Bifrons* Zone).

### **Early phase recovery interval: *Bifrons* Zone, *Commune* Subzone to *Dispansum* Zone**

Following the extinction event, there were no infaunal shelly components for slightly over 2 myr, representing the *Serpentinum* Zone to the lower part of the *Bifrons* Zone (*Commune* Subzone). Levels of ecological tiering increased during the *Bifrons* Zone, with the first significant infaunal component being the deposit-feeding bivalve *D. ovum* (Little 1995; Danise *et al.* 2013; Caswell and Dawn 2019). At this time, small, simple, pyritized feeding traces appeared, indicating an increase in bioturbation in the sediment, and small (1 mm) *Chondrites* burrows were present towards the top of the Alum Shale Member (Martin 2004). Deep infaunal organisms returned shortly after the first appearance of *D. ovum* and were accompanied by a transient reoccurrence of erect epifaunal animals

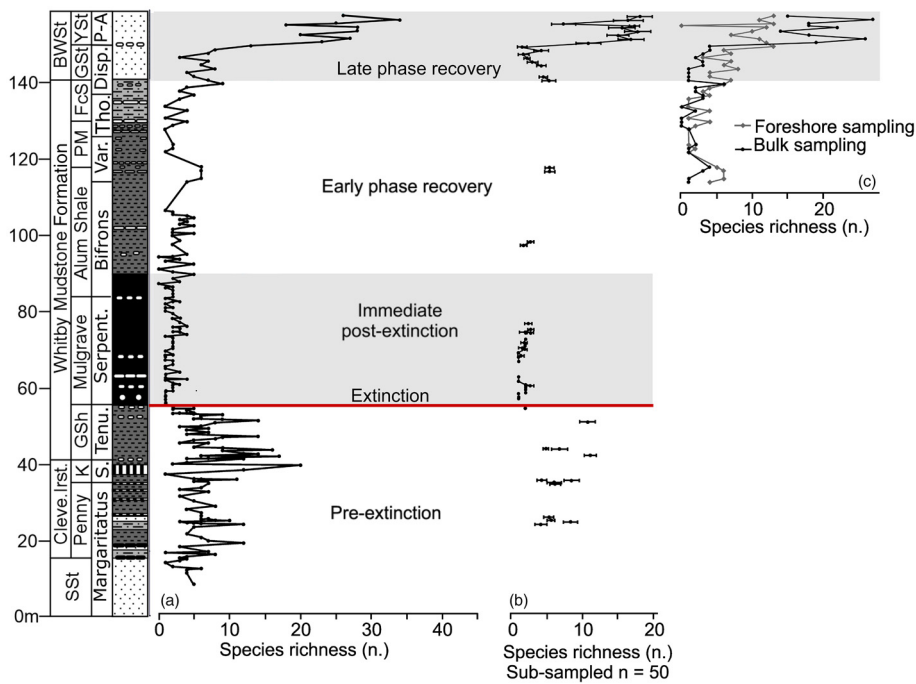


**Fig. 5.** (a) Raw species richness counts per horizon. (b) Subsampled species richness. (c) Foreshore species richness counts (grey diamonds) and species richness counts from bulk-rock samples (black circles). SSt, Staithes Sandstone Formation; Cleve. Irnst., Cleveland Ironstone Formation; BWSt, Blea Wyke Sandstone Formation; Penny, Penny Nab Member; K, Kettleless Member; GSh, Grey Shale Member; Mulgrave, Mulgrave Shale Member; PM, Peak Mudstone Member; FcS, Fox Cliff Siltstone Member; GSt, Grey Sandstone Member; YSt, Yellow Sandstone Member; S., Spinatum Zone; Tenu., Tenuicostatum Zone; Var., Variabilis Zone; Tho., Thoarsense Zone; Disp., Dispansum Zone to Aalensis Zone.

(crinoids). Their presence shows that a tiering structure was briefly restored (albeit following the skeleton crew model) during the Fibulatum Subzone (Bifrons Zone), *c.* 2.7 myr following the extinction event. Until now, this has been the extent of the recovery studied within the Cleveland Basin; above this stratigraphic level, our new results show a continuation of the increasing benthic species richness in both the subsampled data and in the data from bulk collections (Fig. 5).

For the top of the Alum Shale Member, the fluctuation of SID values results from transient, high abundances of the bivalve *M. substriata* (Fig. 6a). The ornate and thick-shelled trigoniid bivalve *Vaugonia literata* is also a common faunal element of the upper Alum Shale Member. The topmost Alum Shale Member marks a temporary highpoint in species richness before a decrease during the subsequent Peak Mudstone and Fox Cliff Siltstone members (Fig. 5a). In much of the Peak Mudstone and Fox Cliff Siltstone members, insufficient specimens were found in both the foreshore and bulk samples to allow for subsampling, which resulted in highly sparse SID values (Fig. 6a, b).

For much of the Peak Mudstone Member (notable for its dark coloration, small rounded phosphatic nodules and pyritized fossil wood), the number of ecologies present and the levels of tiering show a reduction from the underlying Alum Shale, with a temporary loss of both shallow and deep infauna (Fig. 7a). This loss of diversity is recorded in the bulk samples, suggesting that the decline in the Peak Mudstone Member is a true signal and not just an artefact of the generally poor foreshore exposure for most of this unit. This latter fact prevented Martin (2004) from reporting any trace fossils from the Peak Mudstone Member, although small pyritized *Planolites* were encountered during our field collections. Fossil abundances rose through the Fox Cliff Siltstone Member. This was mirrored in the increasing SID values towards a more evenly represented assemblage and a tiering structure similar to that in the upper Alum Shale, with the return of erect epifauna (*Chariocrinus wuerttembergicus*) and both deep and shallow infaunal elements (Fig. 7).

Although species richness increases through the Fox Cliff Siltstone Member, as recorded in both the foreshore and bulk collections, the ecological groups are still only represented by a few species each, resulting in a fluctuating ecological diversity (Fig. 7c). For example,

shallow infaunal suspension feeders from the Fox Cliff Siltstone Member were represented solely by the brachiopod *Lingula beani*, with the previously abundant *V. literata* and *D. ovum* of the upper Alum Shale Member having disappeared from the basin (Fig. 4). Trace

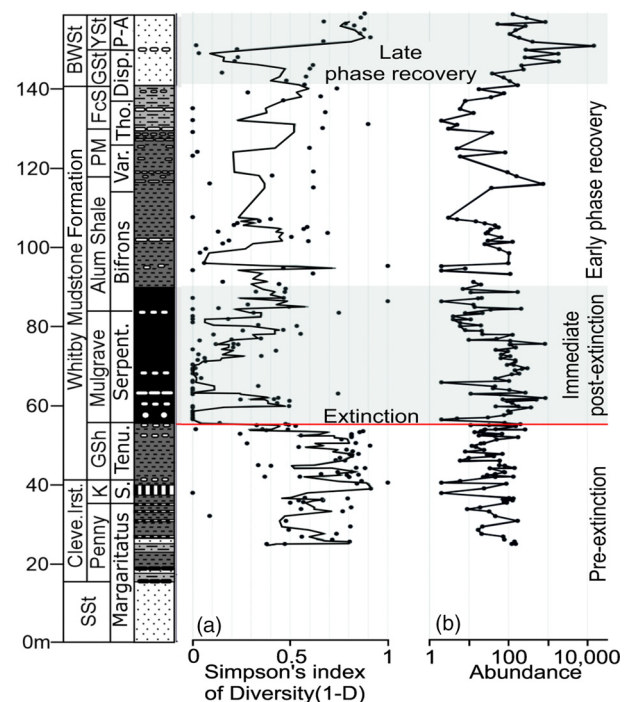


**Fig. 6.** (a) Simpson's index of diversity (1-D) with the three-point moving average trend line. (b) Fossil abundances per horizon. SSt, Staithes Sandstone Formation; Cleve. Irnst., Cleveland Ironstone Formation; BWSt, Blea Wyke Sandstone Formation; Penny, Penny Nab Member; K, Kettleless Member; GSh, Grey Shale Member; Mulgrave, Mulgrave Shale Member; PM, Peak Mudstone Member; FcS, Fox Cliff Siltstone Member; GSt, Grey Sandstone Member; YSt, Yellow Sandstone Member; S., Spinatum Zone; Tenu., Tenuicostatum Zone; Var., Variabilis Zone; Tho., Thoarsense Zone; Disp., Dispansum Zone to Aalensis Zone.

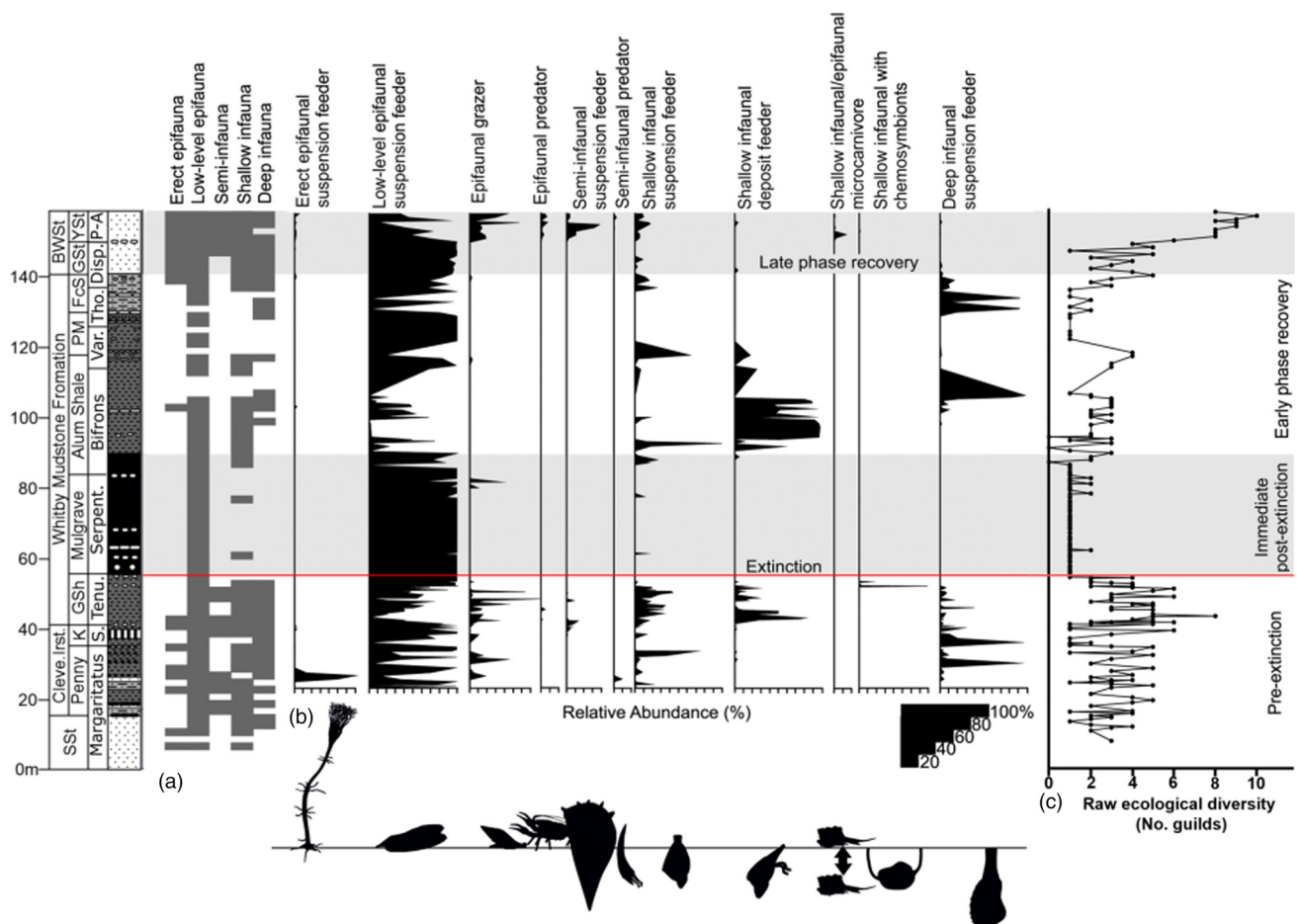


**Fig. 7.** (a) Tiering occupation, dark grey boxes indicate presence of tiering level within 2 m bins of stratigraphy, (b) Contribution, by abundance, of different ecologies per sample horizon, silhouette representative of the different life modes, (c) Total number of ecologies observed per sample horizon, raw ecology counts only. SSt, Staithes Sandstone Formation; Cleve. Irst., Cleveland Ironstone Formation; Penny, Penny Nab Member; K, Kettleless Member; GSh, Grey Shale Member; Mulgrave, Mulgrave Shale Member; PM, Peak Mudstone Member; FcS, Fox Cliff Siltstone Member; GSt, Grey Sandstone Member; YSt, Yellow Sandstone Member; S., Spinatum Zone; Tenu., Tenuicostatum Zone; Var., Variabilis Zone; Tho., Thoarsense Zone; Disp., Dispansum Zone; P-A, Pseudoradosa Zone to Aalensis Zone.

fossil assemblages are represented by *Planolites*, small *Skolithos*-type burrows, *Chondrites* and *Rhizocorallium* (Martin 2001).

#### Late phase recovery interval: Dispansum Zone to Aalensis Zone

This phase saw a marked increase in the number of species present, which resulted in the filling of ecological guilds, a cessation in the fluctuations of ecological diversity that marked the early recovery phases, and the occurrence of a broadly persistent trend towards increased diversity (Fig. 7c). The late phase recovery interval is also coincident with the return of sandy facies within the Cleveland Basin.

Fossil abundances continued to increase, reaching their acme for this section at the top of the Grey Sandstone Member (14 512 counted individuals). This is due to the extreme numbers of the tube worm *Serpula deplexa*, which formed ‘nests’. The abundance of this one species resulted in a sharp and dramatic reduction in the SID value at this level (Fig. 6). The species richness fluctuates throughout the Grey Sandstone Member, although with a greater number of species than the underlying two members. This trend is shown most obviously in the foreshore counts, whereas the bulk sampling shows a progressive increase in the number of species (Fig. 5c). Subsampling shows the converse, suggesting there was a progressive decrease in the number of species. This is probably due to the extremely high numbers of *S. deplexa* swamping the diversity (Fig. 5b). The number of benthic ecologies found within this

member exceeded that typical of the pre-extinction interval (Fig. 7c). The return to sandy facies also marks the return of pedically attached epifaunal brachiopods and a greater level of bioturbation, with *Chondrites*, *Rhizocorallium*, *Taenidium* and large (25 mm diameter) *Thalassinoides* being reported (Martin 2001).

Following the temporary decrease in SID values in the serpulid-rich beds towards the top of the Grey Sandstone Member, there is an increase to stable and high SID values of *c.* 0.82. These are comparable with the pre-extinction interval and indicate a benthic macrofossil assemblage with an even representation of species (Fig. 6a). These high values of SID occur alongside the greatest values of species richness, which increase rapidly at the base of the Yellow Sandstone Member to surpass the pre-extinction values. Around 30 benthic species occur in samples towards the top of the Yellow Sandstone Member, which is *c.* 7 myr after the extinction event (Fig. 5). The Yellow Sandstone Member also contains the greatest number of ecologies of the study interval, with 11 recorded. These include all those present prior to the extinction event (Fig. 7). Within the Yellow Sandstone Member, bulk samples consistently reveal a greater benthic diversity than foreshore sampling (Fig. 5c). This trend is surprising and is explained by the mouldic preservation and small size of many of the specimens, especially gastropods, which were only identifiable after silicon rubber casting and inspection under a microscope. The means that much of the diversity was not appreciated during in-field species counts.

Of the 58 benthic species present in the recovery interval (excluding indeterminate architectibranch and cerithioid gastropods and crustacean limbs), only three species are shared between the post- and pre-extinction assemblages – *Pleuromya costata*, *Oxytoma inequivalvis* and *Meleagrinea substriata* – with only *P. costata* having a prolonged period of absence from the basin. A further 19 taxa are newly occurring species in the basin, but belong to genera that occupied the basin prior to the extinction. Twenty-six species are of genera new to the basin within the study interval.

## Discussion

### *Recovery in the Cleveland Basin and models for recovery*

The post-extinction interval within the Cleveland Basin is here divided into three phases or intervals. The first of these three intervals, the immediate post-extinction interval, spans *c.* 2 myr and, as this interval is represented by low-diversity, high-abundance assemblages with minimal tiering occupation, it could be viewed as a drawn-out survival phase or recovery phase one, following the nomenclature of Kauffman and Erwin (1995) and Twitchett (2006), respectively. It may instead be better to regard this interval as one dominated by low-oxygen specialist communities rather than the onset of true recovery. *B. radiata* and *P. dubius* are often described as opportunistic in their ecology, but an opportunist should be able to colonize a variety of habitats, whereas *P. dubius* in the Cleveland Basin is largely restricted to the organic-rich facies—that is, the Mulgrave Shale Member and the Sulfur Bands of the Grey Shale Member (Little 1995; Caswell and Coe 2013). This facies-dependent model for this species is additionally supported by the decreased abundance of *P. dubius* and its eventual disappearance with improving seafloor ventilation in the Alum Shale Member (Caswell and Coe 2013; Danise *et al.* 2015).

Phases two and three of the Twitchett (2006) recovery model feature an increase in ecological tiering and thereby an increase in ecological diversity. Our early phase recovery interval includes these same features, with the return of shallow and deep infaunal burrowers and erect epifauna. This provides a full suite of the benthic tiering structure *c.* 2.7 myr after the extinction event. However, throughout this interval, each of these tiers is represented by only a few species or a single species, or even a single specimen, and the absence of any of these from an individual sample horizon means that the number of tiers fluctuates. Shortly after the re-establishment of this structure, the diversity decreased and the tiering structure collapsed again during the deposition of the Peak Mudstone Member. However, we did not see a return to *Pseudomytiloides*-dominated assemblages. This interval of decreased diversity is also coincident with a decrease in exposure quality, but because the pattern of diversity was seen in both the bulk collections and the foreshore collections, it is believed to be a genuine signal. A similar trend was recorded by Hallam (1987) for European bivalve species richness per ammonite zone: after an initial increase during the Bifrons Zone, the diversity decreases in the Variabilis Zone.

Our late phase recovery interval features some of the characteristics of recovery stage 4 of Twitchett (2006), with a highly diverse and evenly represented assemblage present for both body and trace fossils. Ecological diversity attained pre-extinction values in the Grey Sandstone Member *c.* 6 myr after the extinction event. This was followed by the filling-out of most guilds, ensuring their presence in each sample horizon and thereby largely removing the fluctuations in ecological diversity seen in the previous phase. This pattern is an important facet of recovery and has been noted during recovery from the Cretaceous–Paleogene, Permian–Triassic and end-Triassic extinction events (Foster and Twitchett 2014; Alvarez *et al.* 2019; Atkinson and Wignall 2019). During this phase, the

species richness exceeded that of the pre-extinction values and we therefore consider this to represent a fully recovered assemblage.

There were, however, several differences in the structure of the recovered assemblage when compared with the pre-extinction interval in the Cleveland Basin. Epifaunal carnivores (e.g. crustaceans and architectibranch gastropods) were represented by three specimens prior to the extinction event, but were of greater significance in the Yellow Sandstone fauna, with up to 8% of fossils from this member belonging to this ecology. For the gastropods, the pre-extinction interval was dominated by vetigastropods with a few caenogastropods, but the upper Toarcian strata were roughly equally dominated by heterobranchs and caenogastropods, with no vetigastropods (Ferrari *et al.* 2020). Within the study interval, crinoids did not regain their former diversity, whereas epifaunal grazers underwent a burst of diversity in the Yellow Sandstone Member that far exceeded the diversity in pre-extinction times. In addition, semi-infaunal suspension feeders occurred at higher relative abundances in the Yellow Sandstone Member than in the pre-extinction interval. This altered structure is also reflected in the relative diversity of the various bivalve orders.

The greatest difference between the pre-extinction interval and the Blea Wkye Sandstone assemblages are that the latter have a comparable lack of diversity within the Pectinida and an increase in Pholadida, despite deep infaunal suspension-feeding organisms being rarer in the recovered assemblages (Fig. 8). Solemyida is lacking from the recovered assemblage, although this is not considered significant as these bivalves were not a part of the normal pre-extinction communities, only being represented by a single species (*Nucinella* sp.) straddling the extinction event. Conversely, several species of bivalves belonging to Trigoniida arrived in the basin during the recovery interval. Little (1995) and Danise *et al.* (2013) did not find any trigonids in the pre-extinction interval, although rare *Liotrignia lingonensis* have been reported from the Spinatum Zone (Morris *et al.* 2019). Trigonids go on to become an important group in the Mid-Jurassic through to the Late Cretaceous (Francis and Hallam 2003). Their paucity prior to the Toarcian extinction event has been noted across much of the British Lower Jurassic (see Supplementary material in Atkinson and Wignall 2020), suggesting that they were still recovering from the end-Triassic extinction event at the onset of the Toarcian event.

The fossil assemblage seen in the upper Toarcian of the Cleveland Basin represents the establishment of typical Mid-Jurassic faunas,

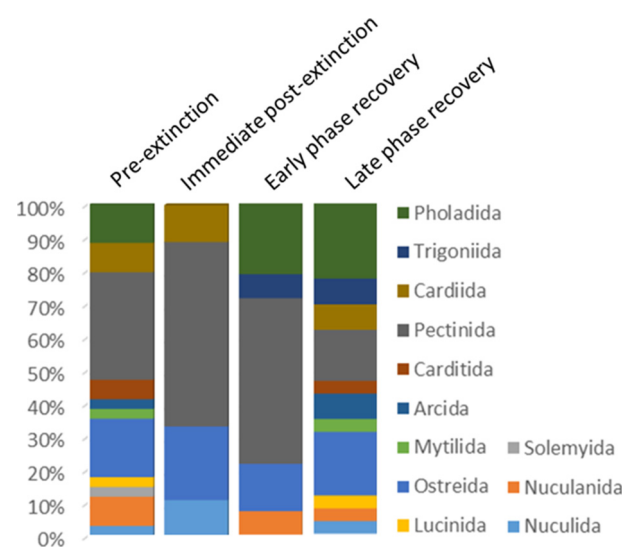


**Fig. 8.** Comparison of proportional diversity within orders of bivalves during pre-extinction, immediately aftermath, early phase recovery and late phase recovery intervals, constructed using raw species data.

with the presence of the bivalves *Pteria plana*, *Goniomya literata*, *Myophorella striata*, and *Actinostreon marshi*, as well as the first representatives of the gastropod families Aporrhaidae, Procerithiidae and Gordenellidae. These taxa all became major faunal components of the Mid-Jurassic (Ferrari *et al.* 2020).

### **Possible causes for the patterns of recovery within the Cleveland Basin**

Palaeo-redox indicators (Re/Mo and Mo/total organic carbon and  $\delta^{98/95}\text{Mo}$ ) suggest that benthic oxygen levels within the Cleveland Basin remained low until the Bifrons Zone, when changes in ocean circulation brought oxygenated Arctic waters south (McArthur *et al.* 2008; Danise *et al.* 2015; Caswell and Frid 2017; van de Schootbrugge *et al.* 2019). This accounts for the >2 myr gap between the extinction and the appearance of *D. ovum*. This interval is also characterized by a marked change in the primary producers, with calcareous nannoplankton and dinoflagellates being replaced by blooms of prasinophyte green algae (Palliani *et al.* 2002; Slater *et al.* 2019). Dinoflagellates begin to increase in relative abundance from the base of the Alum Shale Member, with diversity increasing up through the remaining Whitby Mudstone Formation and into the Blea Wyke Sandstone (Riding 1984; Slater *et al.* 2019; Danise *et al.* 2022). Dinoflagellates are regarded as a better food source for suspension-feeding organisms than green algae as a result of their size and nutrient content (Brown *et al.* 1997; von Elert *et al.* 2003; Wacker and von Elert 2008). Their demise and protracted absence, coupled with persistently low oxygen levels, contributed to the low diversity of suspension-feeding organisms in the Cleveland Basin during our immediate post-extinction interval (Danise *et al.* 2022). This relationship can further be evidenced from the comparably rapid benthic recovery seen in Toarcian successions of the Iberian Range (Spain), where there is no evidence for the development of an anoxic water column and benthic recovery occurred within the Serpentinum Zone (Danise *et al.* 2019).

In the upper portions of the Alum Shale Member, the Th/U ratios indicate increased levels of benthic oxygen (Martin 2001), this being around the time of the first appearance of *D. ovum* within the basin. Caswell and Dawn (2019) suggested *Dacryomya* was tolerant of low-oxygen conditions, allowing it to act as an initial colonizer and to take advantage of organic-rich sediments in areas that were previously anoxic. *Dacryomya ovum* occurs in a narrow stratigraphic interval, perhaps reflecting this requirement for a high organic content within the sediments, a feature needing the correct balance of productivity and low oxygen levels. Caswell and Dawn (2019) suggested that *D. ovum* was an environmental engineer; the action of their burrowing may have acted to oxygenate the substrate, enabling other organisms to subsequently colonize it. It is unclear how significant *Dacryomya* was in the role of opening niches, although its first appearance was shortly followed by the deep infaunal bivalve *Gresslya* and then subsequently crinoids – neither of these would have been excluded by anoxic sediments alone.

A further *c.* 5 myr had elapsed from the first occurrence of *D. ovum* to the fullness of recovery. This stands in contrast with Harries (1999), who, for the Cretaceous–Paleogene and Cenomanian–Turonian extinctions, found that it was the duration of the environmental perturbation that controlled the duration of the ‘survival interval’ and, once this had passed, recovery occurred rapidly. Following the delay to recovery caused by frequent bottom water anoxia during the deposition of the Mulgrave Shale Member, the sluggish recovery thereafter in the Cleveland Basin is attributable to the intervals represented by the Peak Mudstone and Fox Cliff Siltstone members. Species richness was low throughout the Peak Mudstone Member, which is notable for its dark coloration, phosphatic nodules and pyritization of both wood and small simple burrows. These features may indicate that the

Cleveland Basin was again experiencing low levels of oxygen close to the seafloor during this interval. If so, this was not accompanied by a temporary rise in sea-level (Knox 1984).

A later pulse of anoxia would account for the loss of the shallow infaunal species *V. literata* and *D. ovum* and the temporary absence of deep infaunal bivalves until the topmost metre of sediment in this unit. Apart from low-resolution sulfur isotope data, which suggest a continued long-term decrease in pyrite burial in the basin (Newton *et al.* 2011), there are currently no high-resolution redox data available for this interval. However, by the Dispansum Zone, the Th/U values suggest that reoxygenation had occurred (Martin 2004), this also being a time of significant advance in recovery.

The duration of recovery was probably influenced by changes in sea-level. It is notable that the extinction is bracketed by shallow water facies (the Staithes Sandstone, the Cleveland Ironstone and the Blea Wyke Sandstone formations), which host a higher diversity than the intervening deeper water mudstones of the extinction event and the succeeding low-diversity interval (the immediate post-extinction interval). This is not to say that the extinction and recovery are merely an expression of an ordinary water depth–benthic marine diversity gradient with species tracking their preferred habitats (Holland and Patzkowsky 2015; Holland 2020). Had this been the case, then we would expect a far higher number of returning species in the recovered assemblage, rather than only one.

In the intervening 7 myr, it is unlikely that a great many bivalve species would have become extinct as a result of the background extinction rates alone because Jurassic bivalve species have a typical range of 15 ammonite zones (Hallam 1975). It is, however, more likely that recovery occurred faster in the shallower water regions of the Cleveland Basin (Caswell and Coe 2012), with species then tracking their preferred habitat basinwards during shallowing in the mid- and late Toarcian. This could account for the exceptionally long duration of the local recovery. However, the full extent of the control of sea-level on the recovery can only be realized by studying a series of rock sections that would provide a depth transect through the Cleveland Basin across the Toarcian. If such a study is undertaken, then it may reduce the temporal duration of the recovery (Holland 2020).

This idea is supported by the findings of Danise *et al.* (2019) from the Iberian Range of Spain. Their study found that the deeper sections were slightly slower to recover (the Falciferum Subzone rather than the Elegantulum Subzone, equivalent to the Exaratum Subzone; Danise *et al.* 2019). However, it is important to note that these Spanish sections show no evidence of water column anoxia and the interplay of anoxia and sea-level probably caused the overall delay in the Yorkshire successions.

Temperature has been proposed as the main driver of extinction in sections that do not show evidence of the TOAE, but still record the early Toarcian mass extinction event (Danise *et al.* 2019). In the Cleveland Basin, temperature curves have been generated from oxygen isotopes from (mostly) belemnite calcite (Korte and Hesselbo 2011, their supplementary material; Korte *et al.* 2015). These records clearly show the abrupt warming associated with the early Toarcian mass extinction event and the temperatures remained elevated throughout the Serpentinum Zone, but the extent by which the subsequent cooling impacted the duration of the recovery is unclear. Temperatures had begun to decrease by the end of the Serpentinum Zone, but there is a large degree of scatter in the oxygen isotope data, which is attributable to seasonality and the habitat effects of the different belemnite species used. Substantial cooling does not take place until the Aalenian (Mid-Jurassic) (Korte *et al.* 2015, their supplementary material).

### **Comparison with previous studies**

Our findings from the Cleveland Basin add to a developing picture that post-extinction recovery is a mosaic that is highly variable

**Table 1.** Summary of recovery durations for different mass extinction events type of assessment

Event	Location	Recovery duration (myr)	Recovery assessed by	Reference
K-Pg	Antarctica	<1 (Danian)	Stable mollusc diversity	Whittle <i>et al.</i> (2019)
K-Pg	Gulf Coastal Plain, USA	<2 (Danian)	Stable mollusc diversity	Sessa <i>et al.</i> (2009)
K-Pg	Gulf Coastal Plain, USA	c. 2 (Danian)	Ecological structure of mollusc communities	Hansen (1988)
K-Pg	Patagonia	0.5 (Danian)	Offshore mollusc diversity	Aberhan and Kiessling (2014)
K-Pg	Global	10 (Thanetian–Ypresian)	Nannoplankton diversity	Alvarez <i>et al.</i> (2019)
ETME	Europe	c. 2–4 (Sinemurian)	Stable bivalve diversity	Hallam (1987, 1996)
ETME	Global	c. 2–4 (Sinemurian)	Benthic ecosystem function and structure	Dunhill <i>et al.</i> (2018)
ETME	SW Britain	1.26–2.92 (Hettangian)	Benthic tiering structure	Barras and Twitchett (2007), Pugh <i>et al.</i> (2014)
ETME	Tibet	?0.15 (base Hettangian)	High benthic diversity, low dominance and highly specialized forms	Hautmann <i>et al.</i> (2008)
ETME	Argentina	1.26–2.92 (Hettangian)	Stable bivalve diversity	Damborenea <i>et al.</i> (2017)
PTME	Global	50 (Rhaetian)	Marine ecological structure	Song <i>et al.</i> (2018)
PTME	Global	8–9 (Anisian)	Marine ecosystem structure	Chen and Benton (2012)
PTME	Global	<6 (Olenekian)	Bivalve diversity	Ros <i>et al.</i> (2011)
PTME	Hungary	8 (Anisian)	Marine community structure	Foster and Sebe (2017)
PTME	Luoping, China	<10 (Anisian)	Established, complex food webs	Hu <i>et al.</i> (2011)
PTME	Germany and Poland	5–10 (Anisian)	Gastropod species richness	Nützel (2005)

K-Pg, Cretaceous–Paleogene mass extinction; ETME, end-Triassic mass extinction; PTME, Permo-Triassic mass extinction.

between regions and is also dependant on the criteria used to assess recovery. A range of possible recovery durations could be argued for the Cleveland Basin. Based on ecological tiering alone, the recovery spanned <2.7 myr. For ecological diversity to be restabilized, this duration massively increases to c. 6 myr and, using the traditional species counts as the recovery criteria, it is longer still at c. 7 myr. A delayed recovery was also recorded in the trace fossil communities of the Western Tethys Ocean, as evidenced from the Central Western Carpathians of Slovakia (Müller *et al.* 2020). Like the Cleveland Basin, the Serpentinum Zone is marked by a reduced faunal assemblage with the only trace fossils being small and thin and recovery only beginning in the Bifrons Zone. Full pre-extinction diversity is not reattained within their study section, meaning that full recovery exceeds 3.4 myr (Müller *et al.* 2020).

These durations are greater than those in sections from the Sub-Boreal Realm, such as the Iberian and Basque–Cantabrian basins (García Joral *et al.* 2011; Danise *et al.* 2019). In these regions, elevated temperatures may have been the main driving mechanism behind the extinction in the absence of lingering water column anoxia, as seen in the NW European epicontinental basins. The brachiopods faunas recovered by the Variabilis Zone (3.4–4.9 myr after the extinction event) in the Basque–Cantabrian Basin (García Joral *et al.* 2011). Repopulation for brachiopods was faster still in the Iberian Basin, occurring in the Serpentinum Zone (<2 myr after the event), and bivalves were little affected by the extinction (Danise *et al.* 2019).

This pattern of regional differences has similarities with the recovery following the Permian–Triassic mass extinction event, the pace of which was closely related to regional differences in benthic oxygenation. Well-oxygenated Lower Triassic sections commonly feature a level of recovery that would otherwise not have been anticipated until the Mid-Triassic (Twitchett *et al.* 2004; Beatty *et al.* 2008; Hofmann *et al.* 2011; Chen *et al.* 2012; Dai *et al.* 2018). Such regions may also have acted as refuges or origination centres from which species could migrate into other regions once they became habitable again, an idea that has been proposed for migration along the Hispanic Corridor (Hallam 1983; Aberhan 2002).

Large, multi-regional studies conducted using a time-binned approach have previously suggested that recovery from the Toarcian extinction was extremely protracted, extending well into the Mid-Jurassic (Hallam 1996; Ruban 2004). As more local/regional studies

are conducted, this picture is being changed to a more complex mosaic of recoveries occurring at variable rates. For the Cleveland Basin, our longest estimate for the duration for complete recovery is c. 7 myr, which would place the Toarcian recovery as being slower than the recovery from the end-Permian and Cretaceous–Paleogene mass extinctions and on a par with some of the estimates for the Permian–Triassic recovery (Table 1). This is testimony that the intensity of the extinction event is by no means an indication of the duration of recovery (Solé *et al.* 2002). Despite the differences in the magnitudes of the end-Permian and early Toarcian extinction events, there are parallels: both are considered to have been volcanically triggered and involved the spread of oxygen-restricted facies and elevated temperatures. The continuation of harsh environmental conditions has provided one of most plausible theories for why the end-Permian extinction had a protracted interval of low diversity (e.g. Hallam 1991; Foster *et al.* 2018) – a theory that may also be transferable to the Toarcian, with further modulation resulting from changes in sea-level.

## Conclusions

This study documents the full extent and nature of biotic recovery from the early Toarcian mass extinction event within the Cleveland Basin. Benthic oxygen levels remained low following the extinction event, allowing for specialist assemblages tolerant to low oxygen levels to dominate during an interval of high sea-level. These disappeared with improving ventilation and recovery proper was marked by the expansion of infaunal tiers (c. 2 myr post-extinction), followed by epifaunal tiers (c. 2.7 myr post-extinction). Recovery progressed slowly with the temporary absence of infaunal molluscs in the Peak Mudstone Member (straddling the Variabilis and Thoarsense zones), which may have been caused by a return to oxygen-restricted environments. With a continued fall in sea-level and a return to silt- and sand-dominated deposition in the Grey Sandstone Member, the ecological richness matched that of the pre-extinction interval, although many of these ecologies contained only a few species. It was not until the upper Yellow Sandstone Member, when a dramatic increase in species richness occurred, that all the previously present ecologies reappeared and increased diversity facilitated a filling-out of these life modes. The Yellow Sandstone benthic assemblage records the establishment of a typical Mid Jurassic-type assemblage.

Recovery within the Cleveland Basin took at most 7 myr, a duration on par with estimates of recovery rates from the largest mass extinction events of the Phanerozoic. However, recovery within the basin was likely to have been strongly influenced by local sea-levels and the continuation of harsh environmental conditions after the extinction event. To fully appreciate the duration and dynamics of the recovery, a depth transect is required within a single basin, something that is currently unavailable for the Cleveland Basin.

**Acknowledgements** The authors thank Brian Atkinson and Karolina Zarzeczny for their assistance during field collections. We thank Kevin Page, Jean Guex, Andreas Schmidt, Paul Taylor, Robin Knight, Mariel Ferrari, Martin Munt, Carrie Schweitzer and Mike Simms for assistance with resolving some of the taxa within this study. We also thank Silvia Danise and Ian Boomer for providing helpful comments on our paper. Thanks also to Rebecca Bennion for her support and encouragement and for providing comments on an earlier version of this paper.

**Author contributions** JWA: conceptualization (equal), data curation (lead), formal analysis (lead), investigation (lead), writing – original draft (lead); CTSL: conceptualization (equal), supervision (lead), writing – review & editing (lead); AMD: formal analysis (supporting), software (lead), writing – review & editing (supporting).

**Funding** This work was funded by a Geological Society of London undergraduate research bursary in 2013, and The University of Leeds (NERC SPHERES DTP NE/L002574/1).

**Competing interests** The authors declare that they have no known competing financial interests or personal relationships that could have appeared to influence the work reported in this paper.

**Data availability** All data generated or analysed during this study are included in this published article (and if present, its [supplementary information files](#)).

*Scientific editing by Kirsty Edgar*

## References

- Aberhan, M. 2002. Opening of the Hispanic Corridor and Early Jurassic bivalve biodiversity. *Geological Society, London, Special Publications*, **194**, 127–139, <https://doi.org/10.1144/GSL.SP.2002.194.01.10>
- Aberhan, M. and Fürsich, F.T. 2000. Mass origination versus mass extinction: the biological contribution to the Pliensbachian–Toarcian extinction event. *Journal of the Geological Society, London*, **157**, 55–60, <https://doi.org/10.1144/jgs.157.1.55>
- Aberhan, M. and Kiessling, W. 2014. Rebuilding biodiversity of Patagonian marine molluscs after the end-Cretaceous mass extinction. *PLoS One*, **9**, e102629, <https://doi.org/10.1371/journal.pone.0102629>
- Ager, D.V. 1990. *British Liassic Terebratulida (Brachiopoda). Part 1*. The Palaeontographical Society, London.
- Alvarez, S.A., Gibbs, S.J., Bown, P.R., Kim, H., Sheward, R.M. and Ridgwell, A. 2019. Diversity decoupled from ecosystem function and resilience during mass extinction recovery. *Nature*, **574**, 242–245, <https://doi.org/10.1038/s41586-019-1590-8>
- Atkinson, J.W. and Wignall, P.B. 2019. How quick was marine recovery after the end-Triassic mass extinction and what role did anoxia play? *Palaeogeography, Palaeoclimatology, Palaeoecology*, **528**, 99–119, <https://doi.org/10.1016/j.palaeo.2019.05.011>
- Atkinson, J.W. and Wignall, P.B. 2020. Body size trends and recovery amongst bivalves following the end-Triassic mass extinction. *Palaeogeography, Palaeoclimatology, Palaeoecology*, **538**, <https://doi.org/10.1016/j.palaeo.2019.109453>
- Baeza-Carratalá, J.F., García Joral, F., Giannetti, A. and Tent-Manclús, J.E. 2015. Evolution of the last koninckinids (Athyridida, Koninckinidae), a precursor signal of the early Toarcian mass extinction event in the Western Tethys. *Palaeogeography, Palaeoclimatology, Palaeoecology*, **429**, 41–56, <https://doi.org/10.1016/j.palaeo.2015.04.004>
- Bailey, T.R., Rosenthal, Y., McArthur, J.M. and van de Schootbrugge, B. 2003. Paleocceanographic changes of the Late Pliensbachian–Early Toarcian interval: a possible link to the genesis of an oceanic anoxic event. *Earth and Planetary Science Letters*, **212**, 307–320, [https://doi.org/10.1016/S0012-821X\(03\)00278-4](https://doi.org/10.1016/S0012-821X(03)00278-4)
- Bambach, R.K., Bush, A.M. and Erwin, D.H. 2007. Autecology and the filling of ecospace: key metazoan radiations. *Palaeontology*, **50**, 1–22, <https://doi.org/10.1111/j.1475-4983.2006.00611.x>
- Barras, C.G. and Twitchett, R.J. 2007. Response of the marine infauna to Triassic–Jurassic environmental change: ichnological data from southern England. *Palaeogeography, Palaeoclimatology, Palaeoecology*, **244**, 223–241, <https://doi.org/10.1016/j.palaeo.2006.06.040>
- Beatty, T.W., Zonneveld, J.-P. and Henderson, C.M. 2008. Anomalously diverse Early Triassic ichnofossil assemblages in northwest Pangea: a case for a shallow-marine habitable zone. *Geology*, **36**, 771–774, <https://doi.org/10.1130/G24952A.1>
- Brown, M.R., Jeffrey, S.W., Volkman, J.K. and Dunstan, G.A. 1997. Nutritional properties of microalgae for mariculture. *Aquaculture*, **151**, 315–331, [https://doi.org/10.1016/S0044-8486\(96\)01501-3](https://doi.org/10.1016/S0044-8486(96)01501-3)
- Caruthers, A.H., Smith, P.L. and Gröcke, D.R. 2013. The Pliensbachian–Toarcian (Early Jurassic) extinction, a global multi-phased event. *Palaeogeography, Palaeoclimatology, Palaeoecology*, **386**, 104–118, <https://doi.org/10.1016/j.palaeo.2013.05.010>
- Caswell, B.A. and Coe, A.L. 2012. A high-resolution shallow marine record of the Toarcian (Early Jurassic) oceanic anoxic event from the East Midlands Shelf, UK. *Palaeogeography, Palaeoclimatology, Palaeoecology*, **365–366**, 124–135, <https://doi.org/10.1016/j.palaeo.2012.09.021>
- Caswell, B.A. and Coe, A.L. 2013. Primary productivity controls on opportunistic bivalves during Early Jurassic oceanic deoxygenation. *Geology*, **41**, 1163–1166, <https://doi.org/10.1130/G34819.1>
- Caswell, B.A. and Dawn, S.J. 2019. Recovery of benthic communities following the Toarcian oceanic anoxic event in the Cleveland Basin, UK. *Palaeogeography, Palaeoclimatology, Palaeoecology*, **521**, 114–126, <https://doi.org/10.1016/j.palaeo.2019.02.014>
- Caswell, B.A. and Frid, C.L.J. 2017. Marine ecosystem resilience during extreme deoxygenation: the Early Jurassic oceanic anoxic event. *Oecologia*, **183**, 275–290, <https://doi.org/10.1007/s00442-016-3747-6>
- Caswell, B.A., Coe, A.L. and Cohen, A.S. 2009. New range data for marine invertebrate species across the early Toarcian (Early Jurassic) mass extinction. *Journal of the Geological Society, London*, **166**, 859–872, <https://doi.org/10.1144/0016-76492008-0831>
- Chen, Z.-Q. and Benton, M.J. 2012. The timing and pattern of biotic recovery following the end-Permian mass extinction. *Nature Geoscience*, **5**, 375–383, <https://doi.org/10.1038/ngeo1475>
- Chen, Z.-Q., Fraiser, M.L. and Bolton, C. 2012. Early Triassic trace fossils from Gondwana Interior Sea: implication for ecosystem recovery following the end-Permian mass extinction in south high-latitude region. *Gondwana Research*, **22**, 238–255, <https://doi.org/10.1016/j.gr.2011.08.015>
- Cox, L.R., Newell, N. *et al.* 1969. Part N: Bivalvia. In: Moore, R.C. (ed.) *Treatise on Invertebrate Paleontology*. Geological Society of America/University of Kansas.
- Dai, X., Song, H. *et al.* 2018. Rapid biotic rebound during the late Griesbachian indicates heterogeneous recovery patterns after the Permian–Triassic mass extinction. *GSA Bulletin*, **130**, 2015–2030, <https://doi.org/10.1130/B31969.1>
- Damborenea, S.E., Echevarría, J. and Ros-Franch, S. 2017. Biotic recovery after the end-Triassic extinction event: evidence from marine bivalves of the Neuquén Basin, Argentina. *Palaeogeography, Palaeoclimatology, Palaeoecology*, **487**, 93–104, <https://doi.org/10.1016/j.palaeo.2017.08.025>
- Danise, S., Twitchett, R.J., Little, C.T.S. and Clémence, M.-E. 2013. The impact of global warming and anoxia on marine benthic community dynamics: an example from the Toarcian (Early Jurassic). *PLoS One*, **8**, e56255, <https://doi.org/10.1371/journal.pone.0056255>
- Danise, S., Twitchett, R.J. and Little, C.T.S. 2015. Environmental controls on Jurassic marine ecosystems during global warming. *Geology*, **43**, 263–266, <https://doi.org/10.1130/G36390.1>
- Danise, S., Clémence, M.-E., Price, G.D., Murphym, D.P., Gómez, J.J. and Twitchett, R.J. 2019. Stratigraphic and environmental control on marine benthic community change through the early Toarcian extinction event (Iberian Range, Spain). *Palaeogeography, Palaeoclimatology, Palaeoecology*, **524**, 183–200, <https://doi.org/10.1016/j.palaeo.2019.03.039>
- Danise, S., Slater, S.M., Vajda, V. and Twitchett, R.J. 2022. Land–sea ecological connectivity during a Jurassic warming event. *Earth and Planetary Science Letters*, **578**, <https://doi.org/10.1016/j.epsl.2021.117290>
- Dean, W.T. 1954. Notes on part of the upper Lias succession at Blea Wyke, Yorkshire. *Proceedings of the Yorkshire Geological Society*, **29**, 161–179, <https://doi.org/10.1144/pygs.29.3.161>
- Dera, G., Neige, P., Dommergues, J.-L., Fara, E., Laffont, R. and Pellenard, P. 2010. High-resolution dynamics of Early Jurassic marine extinctions: the case of Pliensbachian–Toarcian ammonites (Cephalopoda). *Journal of the Geological Society, London*, **167**, 21–33, <https://doi.org/10.1144/0016-76492009-068>
- Doyle, P. 1990. *The British Toarcian (Lower Jurassic) Belemnites. Part 1*. The Palaeontographical Society, London.
- Dunhill, A.M., Foster, W.J., Sciberras, J. and Twitchett, R.J. 2018. Impact of the Late Triassic mass extinction on functional diversity and composition of marine ecosystems. *Palaeontology*, **61**, 133–148, <https://doi.org/10.1111/pala.12332>
- Erwin, D.H., Valentine, J.W. and Spekoski, J.J. 1987. A comparative study of diversification events: the early Paleozoic versus the Mesozoic. *Evolution*, **41**, 1177–1186, <https://doi.org/10.2307/2409086>
- Ferrari, M., Little, C.T.S. and Atkinson, J.W. 2020. Upper Toarcian (Lower Jurassic) marine gastropods from the Cleveland Basin, England: systematics, palaeobiogeography and contributions to biotic recovery from the early Toarcian extinction event. *Papers in Palaeontology*, **7**, 885–912, <https://doi.org/10.1002/spp2.1322>

- Foster, W.J. and Sebe, K. 2017. Recovery and diversification of marine communities following the late Permian mass extinction event in the western Palaeotethys. *Global and Planetary Change*, **155**, 165–177, <https://doi.org/10.1016/j.gloplacha.2017.07.009>
- Foster, W.J. and Twitchett, R.J. 2014. Functional diversity of marine ecosystems after the Late Permian mass extinction event. *Nature Geoscience*, **7**, 233–238, <https://doi.org/10.1038/NNGEO2079>
- Foster, W.J., Lehmann, D.J., Yu, M., Ji, L. and Martindale, R.C. 2018. Persistent environmental stress delayed the recovery of marine communities in the aftermath of the latest Permian mass extinction. *Paleoceanography and Paleoclimatology*, **33**, 338–353, <https://doi.org/10.1002/2018PA003328>
- Francis, A.O. and Hallam, A. 2003. Ecology and evolution of Jurassic trigoniid bivalves in Europe. *Lethaia*, **36**, 287–304, <https://doi.org/10.1080/00241160310005115>
- García Joral, F. and Goy, A. 2009. Toarcian (Lower Jurassic) brachiopods in Asturias (northern Spain): stratigraphic distribution, critical events and palaeobiogeography. *Geobios*, **42**, 255–264, <https://doi.org/10.1016/j.geobios.2008.10.007>
- García Joral, F., Gómez, J.J. and Goy, A. 2011. Mass extinction and recovery of the Early Toarcian (Early Jurassic) brachiopods linked to climate change in northern and central Spain. *Paleoceanography, Paleoclimatology, Paleoeology*, **302**, 367–380, <https://doi.org/10.1016/j.palaeo.2011.01.023>
- García Joral, F., Baeza-Carratalá, J.F. and Goy, A. 2018. Changes in brachiopod body size prior to the Early Toarcian (Jurassic) mass extinction. *Paleoceanography, Paleoclimatology, Paleoeology*, **506**, 242–249, <https://doi.org/10.1016/j.palaeo.2018.06.045>
- Gómez, J.J. and Goy, A. 2011. Warming-driven mass extinction in the Early Toarcian (Early Jurassic) of northern and central Spain. Correlation with other time-equivalent European sections. *Paleoceanography, Paleoclimatology, Paleoeology*, **306**, 176–195, <https://doi.org/10.1016/j.palaeo.2011.04.018>
- Gradstein, F.M., Ogg, J.G., Schmitz, M. and Ogg, G. 2020. *Geologic Time Scale 2020*. Elsevier.
- Gründel, J., Kaim, A., Nuetzel, A. and Little, C.T. 2011. Early Jurassic gastropods from England. *Paleontology*, **54**, 481–510, <https://doi.org/10.1111/j.1475-4983.2011.01043.x>
- Guxé, J. 1992. Origine des sauts évolutifs chez les ammonites. *Bulletin de la Société Vaudoise des Sciences Naturelles*, **82**, 117–144.
- Guxé, J., Schoene, B. et al. 2012. Geochronological constraints on post-extinction recovery of the ammonioids and carbon cycle perturbations during the Early Jurassic. *Paleoceanography, Paleoclimatology, Paleoeology*, **346–347**, 1–11, <https://doi.org/10.1016/j.palaeo.2012.04.030>
- Hallam, A. 1967. An environmental study of the Upper Domerian and Lower Toarcian in Great Britain. *Philosophical Transactions of the Royal Society London B: Biological Sciences*, **252**, 393–445, <https://doi.org/10.1098/rstb.1967.0028>
- Hallam, A. 1975. Evolutionary size increase and longevity in Jurassic bivalves and ammonites. *Nature*, **258**, 493–496, <https://doi.org/10.1038/258493a0>
- Hallam, A. 1976. Stratigraphic distribution and ecology of European Jurassic bivalves. *Lethaia*, **9**, 245–259, <https://doi.org/10.1111/j.1502-3931.1976.tb01317.x>
- Hallam, A. 1983. Early and Mid-Jurassic molluscan biogeography and the establishment of the central Atlantic seaway. *Paleoceanography, Paleoclimatology, Paleoeology*, **43**, 181–193, [https://doi.org/10.1016/0031-0182\(83\)90010-X](https://doi.org/10.1016/0031-0182(83)90010-X)
- Hallam, A. 1986. The Pliensbachian and Tithonian extinction events. *Nature*, **319**, 765–768, <https://doi.org/10.1038/319765a0>
- Hallam, A. 1987. Radiations and extinctions in relation to environmental change in the marine Lower Jurassic of northwest Europe. *Paleobiology*, **13**, 152–168, <https://doi.org/10.1017/S0094837300008708>
- Hallam, A. 1991. Why was there a delayed radiation after the end-Palaeozoic extinction? *Historical Biology*, **5**, 257–262, <https://doi.org/10.1080/10292389109380405>
- Hallam, A. 1996. Recovery of the marine fauna in Europe after the end-Triassic and early Toarcian mass extinctions. *Geological Society, London, Special Publications*, **102**, 231–236, <https://doi.org/10.1144/GSL.SP.1996.001.01.16>
- Hallam, A. 1997. Estimates of the amount and rate of sea-level change across the Rhaetian–Hettangian and Pliensbachian–Toarcian boundaries (latest Triassic to early Jurassic). *Journal of the Geological Society, London*, **154**, 773–779, <https://doi.org/10.1144/gsjgs.154.5.0773>
- Hallam, A. and Wignall, P.B. 1999. Mass extinctions and sea-level changes. *Earth-Science Reviews*, **48**, 217–250, [https://doi.org/10.1016/S0012-8252\(99\)00055-0](https://doi.org/10.1016/S0012-8252(99)00055-0)
- Hansen, T.A. 1988. Early Tertiary radiation of marine molluscs and the long-term effects of the Cretaceous–Tertiary extinction. *Paleobiology*, **14**, 37–51, <https://doi.org/10.1017/S0094837300011787>
- Harries, P.J. 1999. Repopulations from Cretaceous mass extinctions: environmental and/or evolutionary controls? *GSA, Special Papers*, **332**, 345–364, <https://doi.org/10.1130/0-8137-2332-9.345>
- Harries, P.J., Kauffman, E.G. and Hansen, T.A. 1996. Models for biotic survival following mass extinction. *Geological Society, London, Special Publications*, **102**, 41–60, <https://doi.org/10.1144/GSL.SP.1996.001.01.03>
- Hautmann, M., Stiller, F., Cai, H.W. and Sha, J.-G. 2008. Extinction-recovery pattern of level-bottom faunas across the Triassic–Jurassic boundary in Tibet: implications for potential killing mechanisms. *Palaios*, **23**, 711–718, <https://doi.org/10.2110/palo.2008.p08-005r>
- Hesselbo, S.P., Grocke, D.R., Jenkyns, H.C., Bjerrum, C.J., Farrimond, P., Morgans Bell, H.S. and Green, O.R. 2000. Massive dissociation of gas hydrate during a Jurassic oceanic anoxic event. *Nature*, **406**, 392–395, <https://doi.org/10.1038/35019044>
- Hofmann, R., Goudebrand, N., Wasmer, M., Bucher, H. and Hautmann, M. 2011. New trace fossil evidence for an early recovery signal in the aftermath of the end-Permian mass extinction. *Paleoceanography, Paleoclimatology, Paleoeology*, **310**, 216–226, <https://doi.org/10.1016/j.palaeo.2011.07.014>
- Holland, S.M. 2020. The stratigraphy of mass extinctions and recoveries. *Annual Review of Earth and Planetary Sciences*, **48**, 75–97, <https://doi.org/10.1146/annurev-earth-071719-054827>
- Holland, S.M. and Patzkowsky, M.E. 2015. The stratigraphy of mass extinction. *Paleontology*, **58**, 903–924, <https://doi.org/10.1111/pala.12188>
- Howard, A.S. 1984. *Paleoecology, Sedimentology and Depositional Environments of the Middle Lias of North Yorkshire*. PhD thesis, Queen Mary College, University of London.
- Howard, A.S. 1985. Lithostratigraphy of the Staithes Sandstone and Cleveland Ironstone formations (Lower Jurassic) of north-east Yorkshire. *Proceedings of the Yorkshire Geological Society*, **45**, 261–275, <https://doi.org/10.1144/pygs.45.4.261>
- Howarth, M.K. 1955. Domerian of the Yorkshire coast. *Proceedings of the Yorkshire Geological Society*, **30**, 147–175, <https://doi.org/10.1144/pygs.30.2.147>
- Howarth, M.K. 1962. The Jet Rock series and the Alum Shale series of the Yorkshire coast. *Proceedings of the Yorkshire Geological Society*, **33**, 381–422, <https://doi.org/10.1144/pygs.33.4.381>
- Howarth, M.K. 1992. *The Ammonoite Family Hildoceratidae in the Lower Jurassic of Britain. Part 1*. The Palaeontographical Society, London.
- Hu, S., Zhang, Q. et al. 2011. The Luoping biota: exceptional preservation, and new evidence on the Triassic recovery from end-Permian mass extinction. *Proceedings of the Royal Society London B: Biological Sciences*, **278**, 2274–2282, <https://doi.org/10.1098/rspb.2010.2235>
- Jenkyns, H.C. 1988. The Early Toarcian (Jurassic) anoxic event: stratigraphic, sedimentary, and geochemical evidence. *American Journal of Science*, **288**, 101–151, <https://doi.org/10.2475/ajs.288.2.101>
- Johnson, A. 1984. *The Palaeobiology of the Bivalve Families Pectinidae and Propeamussiidae in the Jurassic of Europe*. Zitteliana, Munich.
- Kauffman, E.G. and Erwin, D.H. 1995. Surviving mass extinctions. *Geotimes*, **14**, 14–17.
- Kauffman, E.G. and Harries, P.J. 1996. The importance of crisis progenitors in recovery from mass extinction. *Geological Society, London, Special Publications*, **102**, 15–39, <https://doi.org/10.1144/GSL.SP.1996.001.01.02>
- Kemp, D.B., Coe, A.L., Cohen, A.S. and Schwark, L. 2005. Astronomical pacing of methane release in the Early Jurassic period. *Nature*, **447**, 396–399, <https://doi.org/10.1038/nature04037>
- Knox, R.W.O. 1984. Lithostratigraphy and depositional history of the late Toarcian sequence at Ravenscar, Yorkshire. *Proceedings of the Yorkshire Geological Society*, **45**, 99–108, <https://doi.org/10.1144/pygs.45.1-2.99>
- Korte, C. and Hesselbo, S.P. 2011. Shallow marine carbon and oxygen isotope and elemental records indicate icehouse–greenhouse cycles during the Early Jurassic. *Paleoceanography*, **26**, 1–18, <https://doi.org/10.1029/2011PA002160>
- Korte, C., Hesselbo, S.P., Ullmann, C., Dietl, G., Ruhl, M., Schweigert, G. and Thibault, N. 2015. Jurassic climate mode governed by ocean gateway. *Nature Communications*, **6**, 10015, <https://doi.org/10.1038/ncomms10015>
- Little, C.T.S. 1995. *The Pliensbachian–Toarcian Event Extinction*. PhD thesis, University of Bristol.
- Little, C.T.S. and Benton, M.J. 1995. Early Jurassic mass extinction: a global long-term event. *Geology*, **23**, 495–498, [https://doi.org/10.1130/0091-7613\(1995\)023<0495:EJMEAG>2.3.CO;2](https://doi.org/10.1130/0091-7613(1995)023<0495:EJMEAG>2.3.CO;2)
- Mander, L., Twitchett, R.J. and Benton, M.J. 2008. Palaeoecology of the Late Triassic extinction event in the SW UK. *Journal of the Geological Society, London*, **165**, 319–332, <https://doi.org/10.1144/0016-76492007-029>
- Martin, K.D. 2001. *Secular Trends in Dysaerobic Trace Fossils*. PhD thesis, University of Leeds.
- Martin, K.D. 2004. A re-evaluation of the relationship between trace fossils and dysoxia. *Geological Society, London, Special Publications*, **228**, 141–156, <https://doi.org/10.1144/GSL.SP.2004.228.01.08>
- McArthur, J.M., Algeo, T.J., van de Schootbrugge, B., Li, Q. and Howarth, R.J. 2008. Basinal restriction, black shales, Re–Os dating, and the Early Toarcian (Jurassic) oceanic anoxic event. *Paleoceanography*, **23**, 1–22, <https://doi.org/10.1029/2008PA001607>
- Miguez-Salas, O., Rodríguez-Tovar, F.J. and Duarte, L.V. 2017. Selective incidence of the Toarcian oceanic anoxic event on macroinvertebrate marine communities: a case from the Lusitanian basin, Portugal. *Lethaia*, **50**, 548–560, <https://doi.org/10.1111/let.12212>
- Milsom, J. and Rawson, P.F. 1989. The Peak Trough – a major control on geology of the North Yorkshire coast. *Geological Magazine*, **126**, 699–705, <https://doi.org/10.1017/S0016756800007007>
- Morris, J. and Lycett, J. 1854. *A Monograph of the Mollusca from the Great Oolite, Chiefly from Minchinhampton and the Coast of Yorkshire. Vol. 3*. The Palaeontographical Society, London.
- Morris, N.J., Knight, R.I., Little, C.T.S. and Atkinson, J.W. 2019. Mollusca – Bivalves. In: Lord, A.R. (ed.) *Fossils from the Lias of the Yorkshire Coast*. The Palaeontological Association, London, 105–157.
- Müller, T., Karancz, S. et al. 2020. Assessing anoxia, recovery and carbonate production setback in a hemipelagic Tethyan basin during the Toarcian Oceanic Anoxic Event (Western Carpathians). *Global and Planetary Change*, **195**, 103366, <https://doi.org/10.1016/j.gloplacha.2020.103366>

- Newton, R.J., Reeves, E.P., Kafousia, N., Wignall, P.B., Bottrell, S.H. and Sha, J.G. 2011. Low marine sulfate concentrations and the isolation of the European epicontinental sea during the Early Jurassic. *Geology*, **39**, 7–10, <https://doi.org/10.1130/G31326.1>
- Nützel, A. 2005. Recovery of gastropods in the Early Triassic. *Comptes Rendus Palevol*, **4**, 501–515, <https://doi.org/10.1016/j.crpv.2005.02.0>
- Page, K.N. 2003. The Lower Jurassic of Europe: its subdivision and correlation. *GEUS Bulletin*, **1**, 21–59, <https://doi.org/10.34194/geusb.v1.4646>
- Palfy, J. and Smith, P.L. 2000. Synchrony between Early Jurassic extinction, oceanic anoxic event, and the Karoo-Ferrar flood basalt volcanism. *Geology*, **28**, 747–750, [https://doi.org/10.1130/0091-7613\(2000\)28<747:SBEJEO>2.0.CO;2](https://doi.org/10.1130/0091-7613(2000)28<747:SBEJEO>2.0.CO;2)
- Palliani, R.B., Mattioli, E. and Riding, J.B. 2002. The response of marine phytoplankton and sedimentary organic matter to the early Toarcian (Lower Jurassic) oceanic anoxic event in northern England. *Marine Micropaleontology*, **46**, 223–245, [https://doi.org/10.1016/S0377-8398\(02\)00064-6](https://doi.org/10.1016/S0377-8398(02)00064-6)
- Payne, J.L. 2005. Evolutionary dynamics of gastropod size across the end-Permian extinction and through the Triassic recovery interval. *Paleobiology*, **31**, 269–290, [https://doi.org/10.1666/0094-8373\(2005\)031\[0269:EDOGSA\]2.0.CO;2](https://doi.org/10.1666/0094-8373(2005)031[0269:EDOGSA]2.0.CO;2)
- Pearce, C.R., Cohen, A.S., Coe, A.L. and Burton, K.W. 2008. Molybdenum isotope evidence for global ocean anoxia coupled with perturbations to the carbon cycle during the Early Jurassic. *Geology*, **36**, 231–234, <https://doi.org/10.1130/G24446A.1>
- Percival, L.M.E., Witt, M.L.I. *et al.* 2015. Globally enhanced mercury deposition during the end-Pliensbachian extinction and Toarcian OAE: a link to the Karoo–Ferrar large igneous province. *Earth and Planetary Science Letters*, **428**, r267–r280, <https://doi.org/10.1016/j.epsl.2015.06.064>
- Powell, J.H. 1984. Lithostratigraphical nomenclature of the Lias Group in the Yorkshire Basin. *Proceedings of the Yorkshire Geological Society*, **45**, 51–57, <https://doi.org/10.1144/pygs.45.1-2.51>
- Powell, J.H. 2010. Jurassic sedimentation in the Cleveland Basin: a review. *Proceedings of the Yorkshire Geological Society*, **58**, 21–72, <https://doi.org/10.1144/pygs.58.1.278>
- Pugh, A.C., Danise, S., Brown, J.R. and Twitchett, R.J. 2014. Benthic ecosystem dynamics following the Late Triassic mass extinction event: Palaeoecology of the Blue Lias Formation, Lyme Regis, UK. *Geoscience in South-West England*, **13**, 255–266.
- Riding, J.B. 1984. A palynological investigation of Toarcian to early Aalenian strata from the Blea Wyke area, Ravenscar, North Yorkshire. *Proceedings of the Yorkshire Geological Society*, **45**, 109–122, <https://doi.org/10.1144/pygs.45.1-2.109>
- Ros, S., De Renzi, M., Damborenea, S.E. and Márquez-Aliaga, A. 2011. Coping between crises: early Triassic–early Jurassic bivalve diversity dynamics. *Palaeogeography, Palaeoclimatology, Palaeoecology*, **311**, 184–199, <https://doi.org/10.1016/j.palaeo.2011.08.020>
- Ruban, D.A. 2004. Diversity dynamics of Early–Middle Jurassic brachiopods of Caucasus, and the Pliensbachian–Toarcian mass extinction. *Acta Palaeontologica Polonica*, **49**, 275–282.
- Ruebsam, W., Mayer, B. and Schwark, L. 2019. Cryosphere carbon dynamics control early Toarcian global warming and sea level evolution. *Global and Planetary Change*, **172**, 440–453, <https://doi.org/10.1016/j.gloplacha.2018.11.003>
- Schmid-Röhl, A., Röhl, H.J., Oschmann, W., Frimmel, A. and Schwark, L. 2002. Palaeoenvironmental reconstruction of Lower Toarcian epicontinental black shales (Posidonia Shale, SW Germany): global versus regional control. *Geobios*, **35**, 13–20, [https://doi.org/10.1016/S0016-6995\(02\)00005-0](https://doi.org/10.1016/S0016-6995(02)00005-0)
- Schubert, J.K. and Bottjer, D.J. 1995. Aftermath of the Permian–Triassic mass extinction event: paleoecology of Lower Triassic carbonates in the western USA. *Palaeogeography, Palaeoclimatology, Palaeoecology*, **116**, 1–39, [https://doi.org/10.1016/0031-0182\(94\)00093-N](https://doi.org/10.1016/0031-0182(94)00093-N)
- Sessa, J.A., Patzkowsky, M.E. and Bralower, T.J. 2009. The impact of lithification on the diversity, size distribution, and recovery dynamics of marine invertebrate assemblages. *Geology*, **37**, 115–118, <https://doi.org/10.1130/G25286A.1>
- Sheehan, P.M. 1985. Reefs are not so different – they follow the evolutionary pattern of level-bottom communities. *Geology*, **13**, 46–49, [https://doi.org/10.1130/0091-7613\(1985\)13<46:RANSDF>2.0.CO;2](https://doi.org/10.1130/0091-7613(1985)13<46:RANSDF>2.0.CO;2)
- Simms, M.J. 1989. *British Lower Jurassic Crinoids*. The Palaeontographical Society, London.
- Slater, S.M., Twitchett, R.J., Danise, S. and Vajda, V. 2019. Substantial vegetation response to Early Jurassic global warming with impacts on oceanic anoxia. *Nature Geoscience*, **12**, 462–467, <https://doi.org/10.1038/s41561-019-0349-z>
- Solé, R.V., Montoya, J.M. and Erwin, D.H. 2002. Recovery after mass extinction: evolutionary assembly in large-scale biosphere dynamics. *Philosophical Transactions of the Royal Society London B: Biological Sciences*, **357**, 697–707, <https://doi.org/10.1098/rstb.2001.0987>
- Song, H., Tong, J. *et al.* 2016. Early Triassic disaster and opportunistic foraminifers in South China. *Geological Magazine*, **153**, 298–315, <https://doi.org/10.1017/S0016756815000497>
- Song, H., Wignall, P.B. and Dunhill, A.M. 2018. Decoupled taxonomic and ecological recoveries from the Permo-Triassic extinction. *Science Advances*, **4**, 1–7, <https://doi.org/10.1126/sciadv.aat5091>
- Sowerby, J. 1821. *The Mineral Conchology of Great Britain or Coloured Figures and Descriptions of Those Remains of Testaceous Animals or Shells, Which Have Been Preserved at Various Times and depths in the Earth*, **3**. W. Arding, London.
- Stanley, G.D. 1988. The history of early Mesozoic reef communities: a three-step process. *PALAIOS*, **3**, 170–183, <https://doi.org/10.2307/3514528>
- Stanley, S.M. 2009. Evidence from ammonoids and conodonts for multiple Early Triassic mass extinctions. *PNAS*, **106**, 15264–15267, <https://doi.org/10.1073/pnas.0907992106>
- Suan, G., Pittet, B., Bour, I., Mattioli, E., Duarte, L.V. and Mailliot, S. 2008. Duration of the Early Toarcian carbon isotope excursion deduced from spectral analysis: consequence for its possible causes. *Earth and Planetary Science Letters*, **267**, 666–679, <https://doi.org/10.1016/j.epsl.2007.12.017>
- Tate, R. and Blake, J.F. 1876. *The Yorkshire Lias*. John Van Voorst, London.
- Twitchett, R.J. 1999. Palaeoenvironments and faunal recovery after the end-Permian mass extinction. *Palaeogeography, Palaeoclimatology, Palaeoecology*, **154**, 27–37, [https://doi.org/10.1016/S0031-0182\(99\)00085-1](https://doi.org/10.1016/S0031-0182(99)00085-1)
- Twitchett, R.J. 2006. The palaeoclimatology, palaeoecology and palaeoenvironmental analysis of mass extinction events. *Palaeogeography, Palaeoclimatology, Palaeoecology*, **232**, 190–213, <https://doi.org/10.1016/j.palaeo.2005.05.019>
- Twitchett, R.J., Krystyn, L., Baud, A., Wheeley, J.R. and Richoz, S. 2004. Rapid marine recovery after the end-Permian mass-extinction event in the absence of marine anoxia. *Geology*, **32**, 805–808, <https://doi.org/10.1130/G20585.1>
- Urbanek, A. 1993. Biotic crises in the history of Upper Silurian graptoloids: a palaeobiological model. *Historical Biology*, **7**, 29–50, <https://doi.org/10.1080/10292389309380442>
- van de Schootbrugge, B., Houben, A.J.P. *et al.* 2019. Enhanced Arctic–Tethys connectivity ended the Toarcian Oceanic Anoxic Event in NW Europe. *Geological Magazine*, **157**, 1593–1611, <https://doi.org/10.1017/S0016756819001262>
- Vasseur, R., Lathuilière, B., Lazăr, I., Martindale, R.C., Bodin, S. and Durlet, C. 2021. Major coral extinctions during the early Toarcian global warming event. *Global and Planetary Change*, **207**, 103647, <https://doi.org/10.1016/j.gloplacha.2021.103647>
- von Elert, E., Martin-Creuzburg, D. and Le Coz, J.R. 2003. Absence of sterols constrains carbon transfer between cyanobacteria and a freshwater herbivore (*Daphnia galeata*). *Proceedings of the Royal Society London B: Biological Sciences*, **270**, 1209–1214, <https://doi.org/10.1098/rspb.2003.2357>
- Wacker, A. and von Elert, E. 2008. Body size and food thresholds for zero growth in *Dressena polymorpha*: a mechanism underlying intraspecific competition. *Freshwater Biology*, **53**, 2356–2363, <https://doi.org/10.1111/j.1365-2427.2008.02051.x>
- Whittle, R.J., Witts, J.D., Bowman, V.C., Crame, J.A., Francis, J.E. and Ineson, J. 2019. Nature and timing of biotic recovery in Antarctic benthic marine ecosystems following the Cretaceous–Palaeogene mass extinction. *Palaeontology*, **62**, 919–934, <https://doi.org/10.1111/pala.12434>
- Wignall, P.B., Newton, R.J. and Little, C.T.S. 2005. The timing of paleoenvironmental change and cause-and-effect relationships during the Early Jurassic mass extinction in Europe. *The American Midland Naturalist*, **305**, 1014–1032, <https://doi.org/10.2475/ajs.305.10.1014>
- Zakharov, V.A., Shurygin, B.N., Il'ina, V.I. and Nikitenko, B.L. 2006. Pliensbachian–Toarcian biotic turnover in North Siberia and the Arctic region. *Stratigraphy and Geological Correlation*, **14**, 399–417, <https://doi.org/10.1134/S0869593806040046>